THE FLORIDA STATE UNIVERSITY

COLLEGE OF ARTS AND SCIENCES

THE MESOSCALE WIND FIELD OVER AN UPWELLING REGION

By
DENNIS L. ELLIOTT

A Thesis submitted to
the Department of Meteorology
in partial fulfillment of the
requirements for the degree of
Master of Science

Approved:

James J. O'Brien
Professor directing Thesis

August, 1974

ABSTRACT

The mesoscale structure of the lowest 1500 m of the atmosphere for the central Oregon coast region is investigated for several case studies during August, 1973.

This study is based primarily on meteorological and sea surface temperature data obtained by an instrumented aircraft; it is supplemented with pilot balloon (pibal), rawinsonde, surface buoy, ship, and land station data.

A description of those field observations is provided. Two different types of aircraft flight patterns were carried out. From 150 m flight level data over the ocean, the horizontal distribution of temperature, dew point temperature, wind velocity, and sea surface temperature are discussed. From a series of horizontal traverses and aircraft soundings made throughout the lowest 1500 m, vertical cross sections of temperature and mixing ratio, extending from 50 km inland to 40 km seaward, are presented for three different cases. A discussion of the wind field is also included.

The most outstanding features observed were an offshore low level jet and a tongue of relatively dry air over the coastal region which appears to be associated with the west end of the sea breeze circulation. The low level jet is revealed to have a structure (or existence) which depends on the basic stratification and depth of the marine layer. It is strictly a mesoscale phenomenon, with width scale of 20-30 km.

depends on the basic stratification and depth of the marine layer. It is strictly a mesoscale phenomenon, with width scale of 20-30 km.

ACKNOWLEDGEMENTS

I am very grateful to my major professor, Dr. James J. O'Brien, for his guidance and inspiration. Dr. C. L. Jordan, Dr. D. E. Pedgley, Dr. J. D. Thompson, Mr. G. A. Dean and Mr. A. J. Johnson deserve many thanks for their consultation and suggestions. Sincere appreciation is extended to Dr. Richard Legeckis, who served as the aircraft flight observer, and to all those people who contributed data from the various aspects of the Coastal Upwelling Experiment to be used for this research. Thanks are also due to Ken Remington and those who assisted in processing the data and to Mr. Dewey Rudd for drafting most of the figures. The Queen Air aircraft was supplied by the Aircraft Facility of the National Center for Atmospheric Research (Boulder, Colorado). The NCAR Computing Facility performed the initial processing of the data. NCAR is sponsored by the National Science Foundation (NSF).

This work was supported primarily by the International Decade of Ocean Exploration (IDOE) through the Coastal Upwelling Ecosystems Analysis (CUEA) program under NSF Grant No. GX-33502. The Office of Naval Research, Ocean Science and Technology Branch, provided partial support.

TABLE OF CONTENTS

TABLE OF CONTENTS - Continued

LIST OF TABLES

LIST OF ILLUSTRATIONS

10. Same as Fig. 9 except for air temperature, dew point temperature, and sea surface temperature for 18 August 1973 . 27

LIST OF ILLUSTRATIONS - Continued

1. INTRODUCTION

As part of the Coastal Upwelling Experiment (CUE II) off the central Oregon coast during the summer of 1973, an extensive meteorological program was carried out. An overall objective of this program was to gain an increased understanding of the winds producing the coastal upwelling phenomenon and of the mesoscale interaction of the atmosphere and the ocean.

This study is based primarily on aircraft data, supplemented with rawinsonde, pibal, surface buoy, ship, and land station data taken during CUE II. The mesoscale region of study extended from approximately 40 km seaward to 50 km inland and about 100 km in the north-south direction. A total of 27 aircraft flights were made during the month of August. Never before has such an extensive mesoscale meteorological study been conducted over a coastal upwelling region. Aerial explorations on a much larger scale have been made off the coast of Somalia, another upwelling region, to investigate the cross equatorial jet of the western Indian Ocean (Bunker, 1965; Findlater, 1972). Most previous studies have been in terms of the spatial and/or time variations of surface winds (Burt et al., 1972, 1973; Maeda and Kishimoto, 1970).

The summer climate off the Pacific coast of the United States is dominated by the presence of a large sea level Pacific anticyclone. Intense daytime heating inland produces a large-scale gradient wind flow dominated by the presence of a large sea level Pacific anticyclone. Intense daytime heating inland produces a large-scale gradient wind flow along the coast. This sustained northerly flow along the coast acts to

increase the coastal upwelling, thus reducing the nearshore sea surface temperatures. A strong coastal thermal gradient results from the intense heating inland and cold surface waters, leading to the development of a sea breeze circulation. Johnson and O'Brien (1973) have investigated an Oregon sea breeze event for a case study in August 1972 from the coast to 60 km inland. The need for an expanded meteorological program was realized, as little was known about the seaward variation of the mesoscale wind field over an upwelling region. Questions such as: "How does the sea surface temperature pattern relate to the low level wind field?", and "What is the seaward extent of the sea breeze circulation?" have long remained unanswered due to lack of sufficient data over the upwelling region.

The main purpose of this study is to attempt to evaluate the character of the low level, mesoscale, horizontal wind field over the upwelling region off the central Oregon coast. Low level refers to the lowest 1.5 km; it might be pointed out, however, that the majority of aircraft observations were made at 150 m flight level. In an effort to determine more knowledge of the physical processes involved, the kinematic structure of the wind field is examined with consideration of the stability, marine layer depth, sea surface temperature, and sea breeze circulation.

Case studies are selected as being representative of the mean summer climatology for the Oregon coast region. Cases which include major synoptic events, such as the occurrence of moderate to strong southerly

mer climatology for the Oregon coast region. Cases which include major
synoptic events, such as the occurrence of moderate to strong southerly winds associated with a large scale frontal system, are not considered here.

In the following sections of this paper, a complete description of the meteorological program and a discussion of the mesoscale phenomena observed for several case studies will be presented. Section 2 describes the field observations during CUE II and includes the methods used in the data analysis. A discussion of mesoscale features observed during 150 m (500 ft) flight level patterns - focusing on the occurrence of an offshore low level wind speed maximum - is given in Section 3. In Section 4, the vertical structure of temperature, moisture, and wind for the lowest 1500 m, extending from 40 km seaward to 50 km inland, is discussed for three different cases. The summary and conclusions are presented in Section 5.

2. FIELD OBSERVATIONS

Meteorological data for this study came from a variety of sources, including aircraft, rawinsondes, pibals, buoys, ships, and coastal land stations. The majority of the analyses are based on aircraft data, supplemented with data from the other sources. A summary listing of data collected during CUE II has been compiled by Pillsbury and O'Brien (1973).

a. Aircraft observations

During the month of August 1973, the NCAR Queen Air aircraft participated in CUE II off the central Oregon coast. The aircraft was equipped with a remote infrared thermometer for measuring sea surface temperatures and instruments for measuring meteorological parameters, such as wind velocity, air temperature, dew point temperature, pressure, liquid water content, and the color photography of the sea surface. A Doppler navigation system was used in measuring wind velocities.

Two different types of flight patterns were carried out by the Queen Air. During Type I, the aircraft flew low-level flight tracks at 152 m (500 ft) above the ocean, as the determination of the horizontal structure of the sea surface temperature field was the primary objective. The grid area extended 30-40 km offshore from Siletz Bay to Point Garibaldi. Fig. 1 shows a typical flight pattern. From C (triangle), the aircraft usually flew south to Salishan and covered the southern part of the study area first. Occasionally, changes in the flight pattern were made due to fog or the need to make a pass over a ship. The reason for

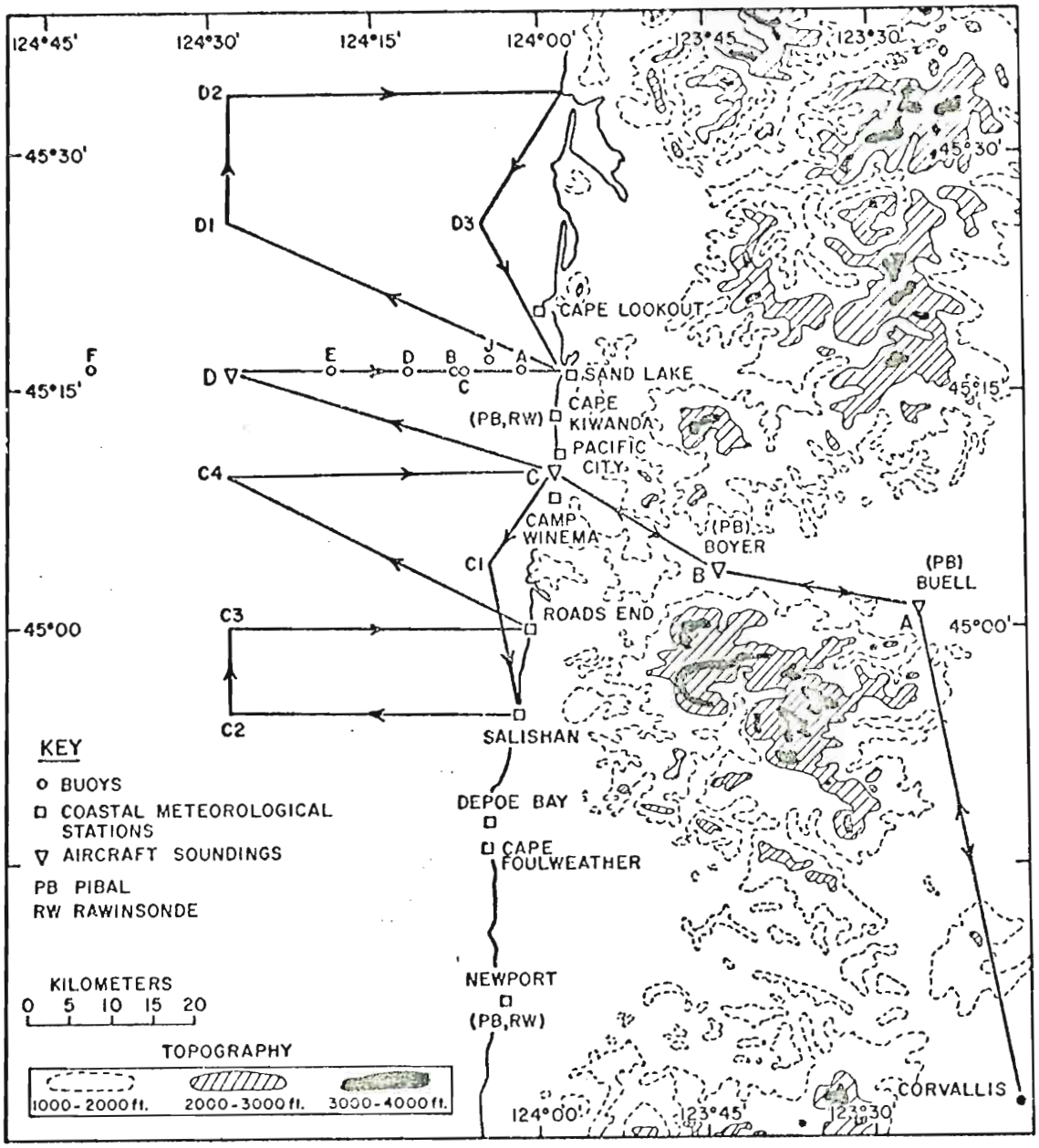

Fig. 1. Map of central Oregon coast showing the NCAR aircraft flight pattern and meteorological observing stations

Fig. 1. Map of central Oregon coast showing the NCAR aircraft flight pattern and meteorological observing stations during CUE-II.

passing over a ship was to obtain a reference sea surface temperature measure from shipboard, which is referred to as ground truth, to test the aircraft's calibration. A report on the preparation of sea surface temperature maps from CUE II is given by O'Brien et al. (1974). Meteorological aircraft soundings were obtained near Pacific City (C triangle); offshore (D triangle) at approximately 40 km from Sand Lake; and at two positions located about 25 km and 50 km inland. During each vertical sounding, the aircraft made a spiral descent (or the opposite spiral ascent) from 1524 m (5000 ft) to 152 m (500 ft) over the ocean and to 457 m (1500 ft) over land.

During Type II flights (Fig. 2), the aircraft collected meteorological data by flying horizontal traverses at altitudes of 305 m (1000 ft) to 1524 m (5000 ft) in steps of 305 m (1000 ft) from approximately 50 km inland to 40 km seaward. Vertical soundings were made at points A, B, C, and D indicated by triangles. (Note that A, B, C, and D circles are ocean buoys--not aircraft soundings.)

In addition to Type I and II flights, there were two special flights. On 4 August, a flight collected ground-truth data for Skylab mission #0841 and on 18 August a flight was made 140 km westward along the buoy line off Sand Lake. The data from the 18 August flight were very interesting. A distinct wind speed maximum was observed at approximately 20-30 km offshore and was associated with a pronounced horizontal gradient in dew point temperature. The description of these low level atmospheric phenomena is a major objective of this paper.

perature. The description of these low level atmospheric phenomena is a major objective of this paper.

All meteorological and infrared measured sea surface temperature data were recorded on magnetic tape with the NCAR ARIS system during the

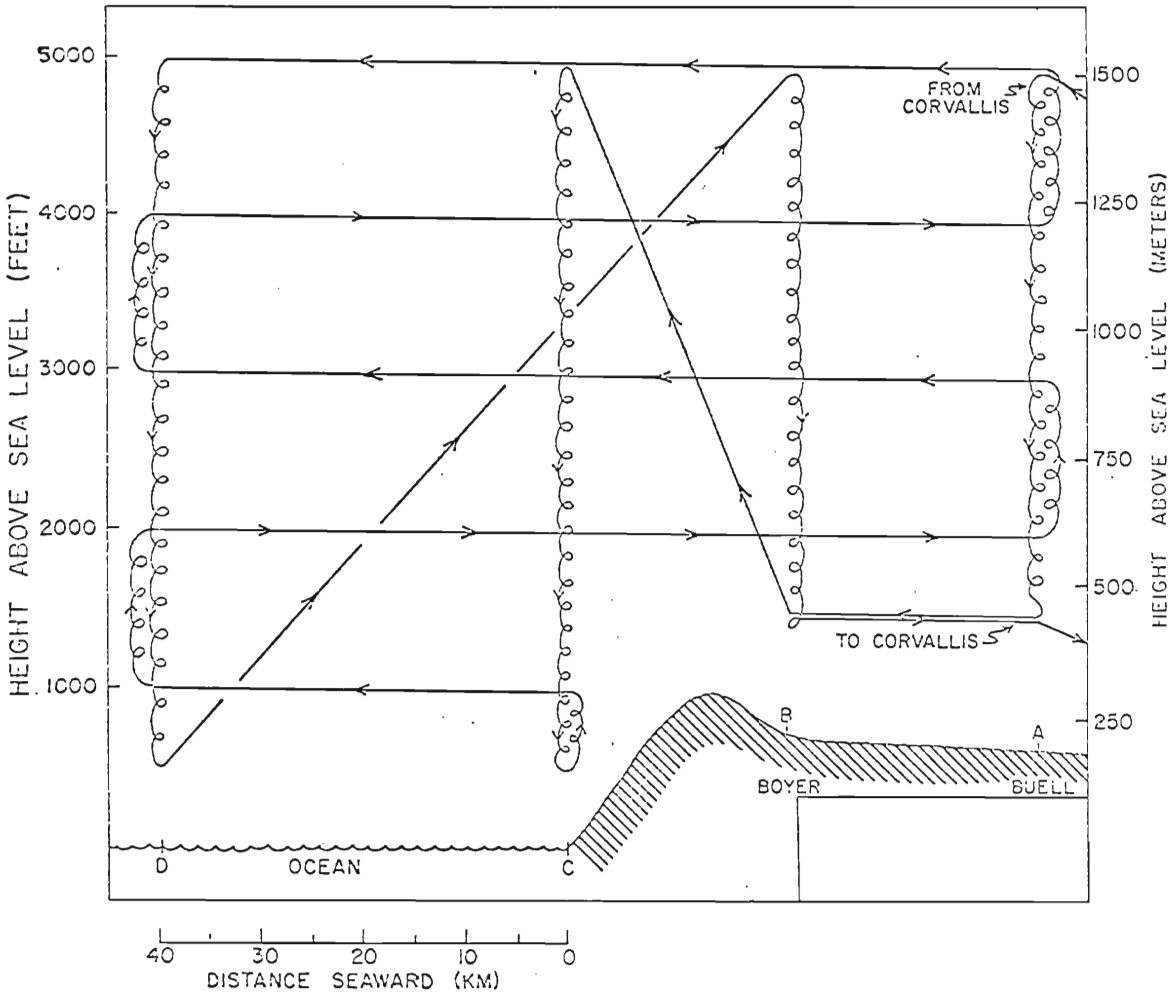

Fig. 2. Type II flight pattern of the NCAR aircraft during CUE-II. Refer to Fig. 1 for location of the soundings.

flights. At the end of the project, the tapes were processed by the NCAR Aircraft and Computer Facilities. From a continuous record, the wind data were read and plotted in half-minute intervals for Type I and one minute intervals for Type II along each flight leg. For these plots, aircraft speed was approximately 75 m sec^{-1}, so that each minute corresponds to about 4.5 km. All Doppler winds computed from the ARIS data were utilized except those data obtained during spiral descents, sharp turns, and other times when the Doppler gave unreliable winds. When the ocean surface was relatively calm the Doppler system would go into memory, giving unreliable winds. A summary on the accuracy of Doppler winds and data errors is given at the end of this section.

b. Pibal and rawinsonde observations

During the latter part of August, an observational program was carried out by D. W. Stuart, and his team, to gain additional meteorological data. Rawinsondes were launched every six hours at 0500, 1100, 1700, and 2300 PDT on 18-19, 22-23, and 26-27 August at Cape Kiwanda and Salem. Pibals were launched every 2 hours, day and night, for the same periods at the Marine Science Center in Newport, at Boyer and Buell, and at Cape Kiwanda and Salem except during times of rawinsonde launches. In addition, transpondersondes released from the ship R/V CAYUSE, were tracked from near Cape Kiwanda. Balloon positions from all releases were recorded each half-minute of flight yielding wind observations for approximately every 100 m. Each sounding was terminated after 30 minutes of flight.

recorded each half-minute of flight yielding wind observations for approximately every 100 m. Each sounding was terminated after 30 minutes of flight.

The NCAR Queen Air aircraft flew both Type I and II flights each of these days, except for flight #12 on the 18th when a special flight

140 km seaward was made. In most cases, the aircraft tried to schedule its soundings for Cape Kiwanda at approximately the same time as a pibal or rawinsonde release.

Pibals also were released twice daily at Cape Kiwanda from 9-30 August and at Newport from 1-31 August. Pibal and rawinsonde data were used mainly as a check and supplement to the aircraft flight data.

c. Surface observations

Surface meteorological data were collected from offshore buoys, ships, and numerous land stations. Winds, air temperature, and sea surface temperature were recorded at nine buoys, extending out to 150 km along the Sand Lake buoy line. Figure 1 shows the location of these buoys, labelled with letters; buoy G was located at 125W and H near 125.5W at approximately the same latitude. Buoys D, F, G, and J were without wind direction measurements.

Ships participating in CUE II were NOAA Ship OCEANOGRAPHER (Seattle, WA), R/V Thomas G. Thompson (U. of Washington), and R/V's CAYUSE and YAQUINA (Oregon State University). Routine meteorological observations were made by the ships in addition to their oceanographic observations.

A total of 27 surface stations, from the coast to approximately 60 km inland, also provided meteorological data.

d. Comments on data errors and the accuracy of Doppler winds

In this section we describe the type of errors observed in the data. Errors were of two main types: (1) FM radio interference and (2) Doppler wind errors.

Early in the field operations, it was determined that the FM

radio influences the data signal during voice transmissions. For this reason, the radio usage was noted in the observer's flight log. Interference usually appeared in the form of spikes, and affected temperature, dew point temperature, and sea surface temperature readings. Effects of radio usage on wind speed and direction were not always obvious. Usually, the interference occurred over a time interval of less than two minutes. (Two minutes corresponds to about 9 km.) Linear interpolation was employed to estimate the data in areas of interference.

Although no experiments were carried out in this project to determine the accuracy of the Doppler winds, extensive aircraft calibrations and intercomparison studies have been conducted by the National Hail Research Experiment (NHRE) group and others. Duchon et al. (1972) gives a concise summary of this program, while a more intensive discussion is provided in NHRE (1972). Recent information on the instrumentation and characteristics of the Queen Air aircraft is available (Burris et al., 1973).

Foote and Fankhauser (1973) discuss the accuracy of winds measured by the Queen Air, which utilizes a Doppler navigation system. The Doppler system was compared with the inertial navigation system, which was taken as the standard. For wind speeds of at least 5 m sec^{-1}, mean-value differences were found to be less than 1 m sec^{-1} in wind speed and 10^{o} in wind direction. For higher wind speeds, these differences decreased. A cross-spectral analysis comparing Doppler winds with inertial winds indicates there is no significant correlation for scales < 3-4 km.

A cross-spectral analysis comparing Doppler winds with inertial winds indicates there is no significant correlation for scales < 3-4 km.

During CUE II, most of the flight time was over the ocean, which is a moving surface. Since, however, wind velocities are generally two orders

of magnitude larger than surface velocities of the ocean, the influence of ocean surface velocities were neglected.

During Type I flights, a slight shift in the magnitude and direction of Doppler winds was noted between north-south and east-west legs. Directional shifts ranged from 10°-20°. Wind speeds measured along N-S legs were generally 1.2-1.6 times greater than those along E-W legs. However, no shifts were apparent between flights of opposite direction (180° different). For example, note the winds observed from the special seaward flight that was carried out during the afternoon of 18 August. Seaward, where the difference in time was less, there were no apparent shifts in either wind speed or direction. Moreover, during nearly all of the August flights, wind data were found to be consistent along flight legs of the same (or exact opposite) aircraft heading. That is, wind data measured along easterly flight headings were consistent with those along westerly headings, and wind data measured along northerly headings consistent with those along southerly headings.

Relative speed and directional changes along each leg agreed with relative changes along other legs. Over the upwelling region, the relative changes in wind speed and direction were greatest along E-W flight legs. For this reason, absolute values along E-W legs were taken as standard, while relative changes along other legs were utilized to provide greater continuity over the study area.

3. THE HORIZONTAL DISTRIBUTION OF MOISTURE, TEMPERATURE, AND WIND

Perhaps the most surprising meteorological feature observed during CUE II was the occurrence of a low level wind speed maximum offshore. As the offshore wind speed maximum appears quite significant, we will often refer to it as a jet. From 152 m (500 ft) flight level data, the jet was observed 15-25 km offshore. In this section we present a summary of aircraft wind data available to us during August 1973 and describe the mesoscale synoptic situation for 3 separate days with Type I flights. Data from Type II flights will be presented and discussed in Section 4.

Table I lists all of the aircraft flights and the wind speeds and directions observed for each flight. From a total of 27 flights, 12 were utilized for studying the mesoscale wind field. Out of these 12, three showed an offshore wind speed maximum, five showed a decrease of wind speed seaward, and four revealed no pronounced changes in wind speed. The other 15 cases were not utilized for one or more of the following reasons: (1) light and variable winds; (2) an unfavorable synoptic situation, i.e., a large-scale front or low pressure system; (3) unreliable Doppler winds; or (4) an incomplete flight pattern.

A brief description of the overall wind pattern for each low level flight is included with the comments in Table I. Temperature and dew point temperature fields for Type I flights were investigated but analyzed only for cases with significant changes in the pattern. The pattern was very

temperature fields for Type I flights were investigated but analyzed only for cases with significant changes in the pattern. The pattern was very

uniform in most cases, with only 1-2C change over the entire study area.

Table I -- Summary of Queen Air aircraft flights and winds observed over the upwelling region during CUE-II.

Date	Flight	Type	Start	Wind Speed ($m\ sec^{-1}$)	Wind Direction	Comments
Aug. 1	1*	II	10:38	8-12	NNE-NNW	Fog offshore
2	No Flight-Fog					
3	2*	I	13:05	8-13	NNE-NNW	Largest wind speeds from coast to 30 km seaward.
4	3	Special Support Sky Lab	8:42	----	----	----
		I	11:04	2-10	NNE-NNW	Approaching front; rain, clouds NW part of study area.
5	4	I	9:40	----	----	Flat ocean. Doppler in memory.
6	No Flight-Fog					
7	5	II	8:55	----	----	Short flight due to Doppler in memory over flat ocean.
8,9,10,11	No Flights-Scheduled down					
12	6	II	9:55	----	----	Doppler in memory most of flight over ocean.
13	7	II	13:32	----	----	Incomplete flight pattern due to low clouds and fog.
14	8*	I	12:57	6-8.5	N-NNW	Wind speed decreases seaward.
15	9*	I	10:02	3-6	NNE-N	Wind speed decreases seaward.
16	No Flight					
17	10	I	10:21	2-4	NE-NNW	Areas of flat ocean. Doppler occasionally goes into memory.
						Areas of flat ocean. Doppler occasionally goes into memory.

Table I, continued

Date	Flight	Type	Start	Wind Speed ($m\ sec^{-1}$)	Wind Direction	Comments
Aug. 18	11*	I	8:53	1.5-5.5	NNE-NNW	Wind speed maximum 10-20 km offshore. Sharp horiz. moisture gradient offshore.
	12*	Special	13:27	4-7.5	NNE-NNW	Wind speed maximum 20-30 km offshore. Sharp horiz. moisture gradient offshore.
19	13	II	9:09	____	____	Incomplete flight pattern. Doppler frequently in memory.
	14*	I	13:32	2-5	N-WNW	____
20	15*	I	12:30	2-5	NNE-NW	Wind speed decreases seaward.
21	16	I	11:22	Light and variable		____
22	17	I	8:57	Light and variable		Flat ocean. Doppler frequently in memory.
	18	II	13:38	Light and variable		Doppler frequently in memory over ocean.
23	19	I	8:58	1-4	S-WSW	Approaching synoptic scale cyclone.
	20	II	13:19	1-6	S-SW	Altered flight pattern due to clouds.
24	No Flight-Overcast and Rain					
25	21*	I	12:21	3-6.5	NNW-NW	Wind speed maximum 15-20 km offshore. Sharp horiz. moisture gradient offshore.
26	22*	I	9:08	2-6	NE-NNW	Wind speed decreases seaward.
	23*	II	15:49	5-7	N-NW	Doppler occasionally in memory over ocean.
	23*	II	15:49	5-7	N-NW	Doppler occasionally in memory over ocean.

Table I, continued

Date	Flight	Type	Start	Wind Speed ($m\ sec^{-1}$)	Wind Direction	Comments
Aug. 27	24	I	8:55	Light and variable		Flat ocean. Doppler frequently in memory.
	25	II	15:54	____	____	Flat ocean. Doppler frequently in memory.
28	26	I	8:54	Light and variable		Flat ocean. Doppler frequently in memory.
29	27*	I	9:04	2-5	NE-NNW	Largest wind speeds in southern half of study area.

*Indicates those flights utilized in studying the mesoscale wind field.

It is interesting to note that the largest horizontal temperature and dew point gradients were found in regions of offshore wind speed maximum. We present two cases with offshore wind speed maximum and one case where the wind speed decreases seaward.

a. Case of 25 August

On 25 August, a distinct low level wind speed maximum was observed from 15-20 km offshore, oriented almost parallel to the coast line (Fig. 3). A wind speed minimum occurred near 10 km offshore. In the southern half of the study area, the isogon pattern (Fig. 4) shows directional confluence ahead of the speed maximum and directional difluence associated with the speed minimum. There is no evidence of an offshore jet at the surface, based upon an investigation of buoy and ship winds for 25 August.

In order to determine whether or not the offshore jet is associated with a large scale frontal zone or any other synoptic events, it is necessary to investigate the synoptic scale pattern. Figs. 5 and 6 show the synoptic pattern for the Pacific coast at the surface and 850 mb for 1700 PDT 25 August. A front lies about 600 km to the west of the central Oregon coast but has no effect on the mesoscale wind field near the coast. With the large high pressure system over the eastern Pacific Ocean and the thermal trough extending northward from California, the synoptic scale pattern here is quite typical for the Pacific coast during August. The weak low pressure system in eastern Washington is the remnant of a surprisingly intense storm which struck the Oregon coast on 24 August. With the passage of the low and the extension of the high pressure cell inland, north-

intense storm which struck the Oregon coast on 24 August. With the passage of the low and the extension of the high pressure cell inland, north-

erly winds returned to the coast bringing on an upwelling event. With the return of northerly winds, the coastal upwelling process was initiated again. Oceanographers refer to this initiation and maintenance of upwelling as an

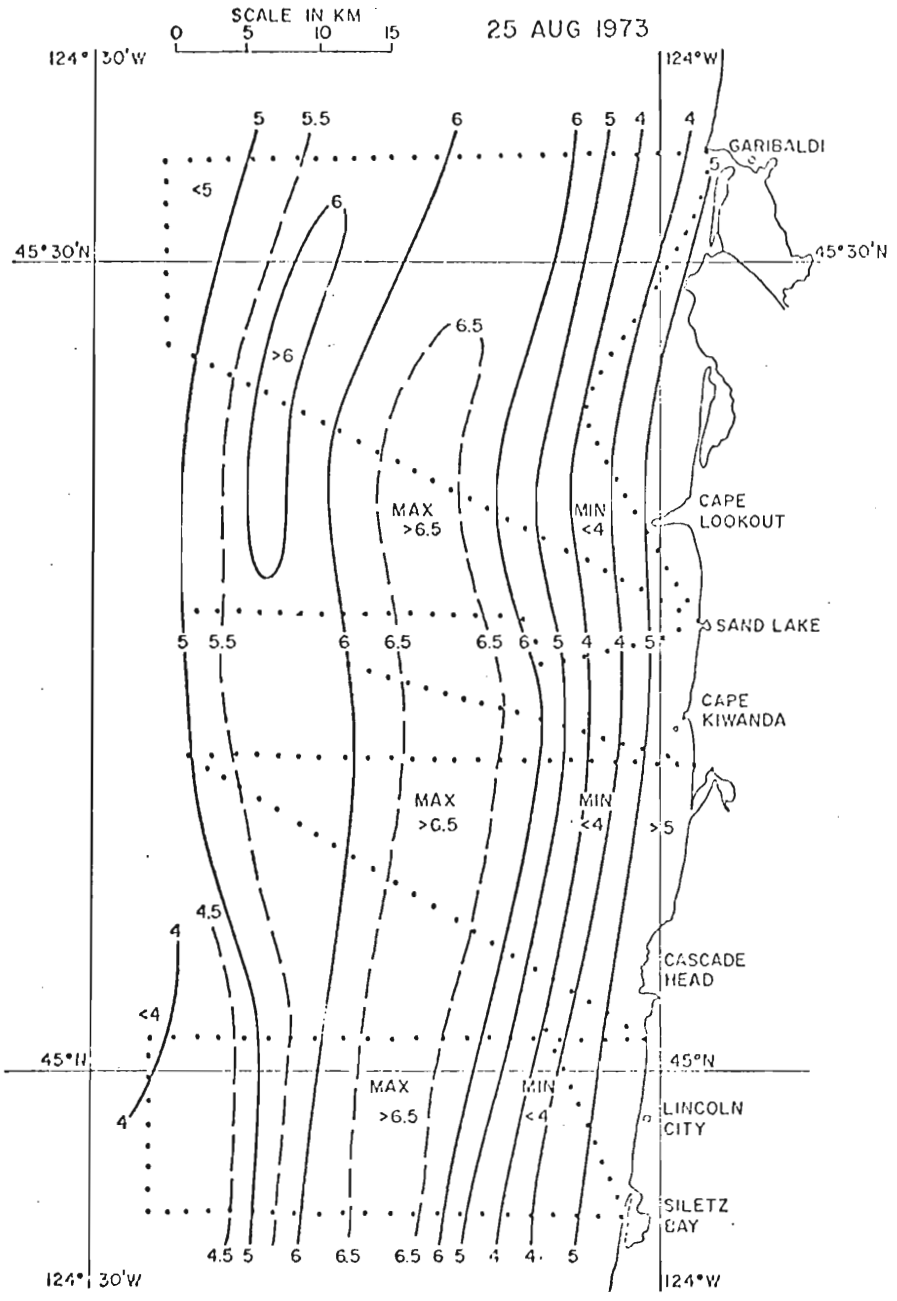

Fig. 3. Isotachs of wind speed (m sec^{-1}) at 152 m (500 ft) for the period 1300-1500 PDT 25 Aug 1973. Dotted lines show the aircraft flight pattern.

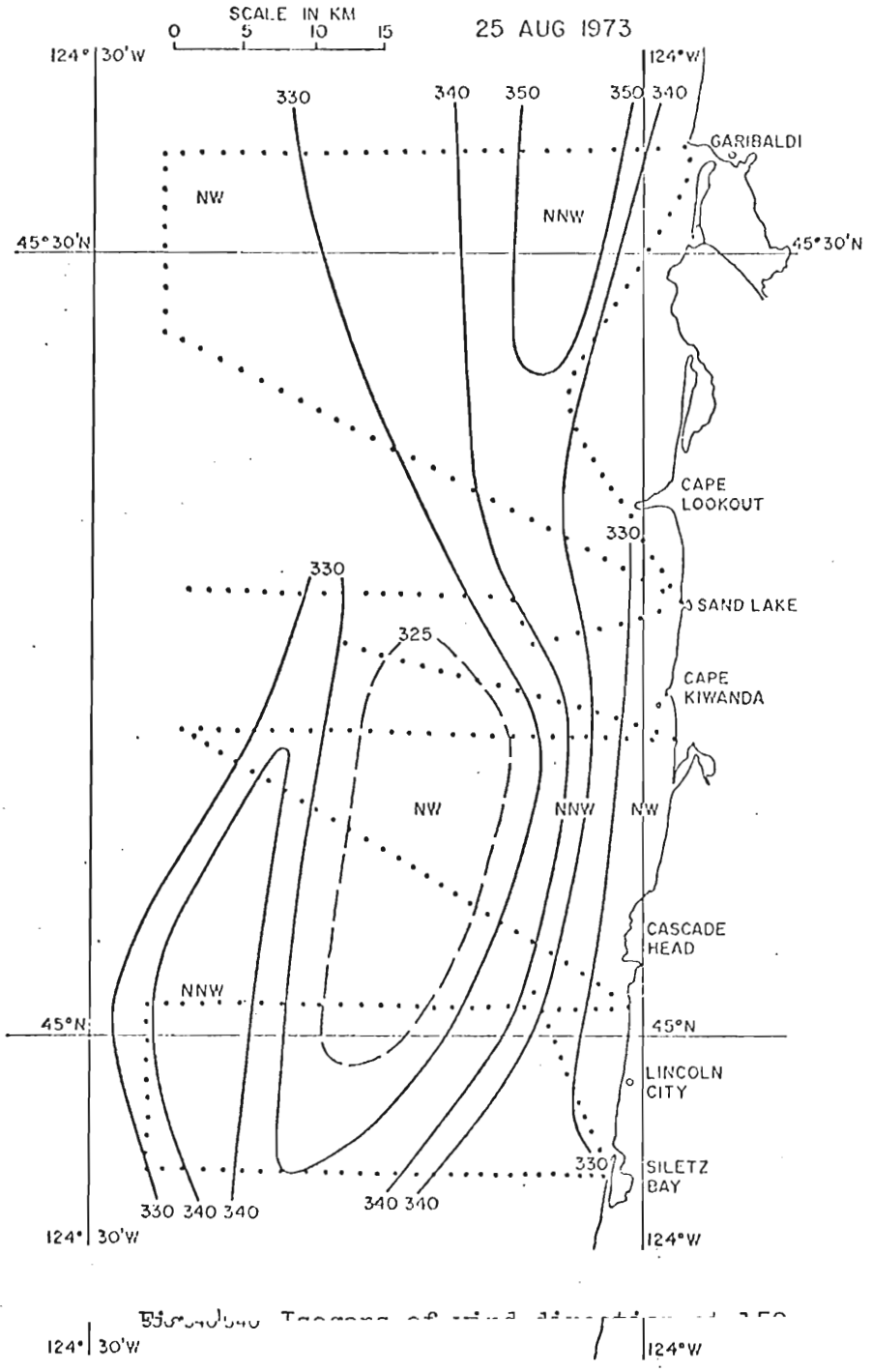

Fig. 4. Isogons of wind direction at 152 m (500 ft) for the period 1300-1500 PDT 25 Aug 1973.

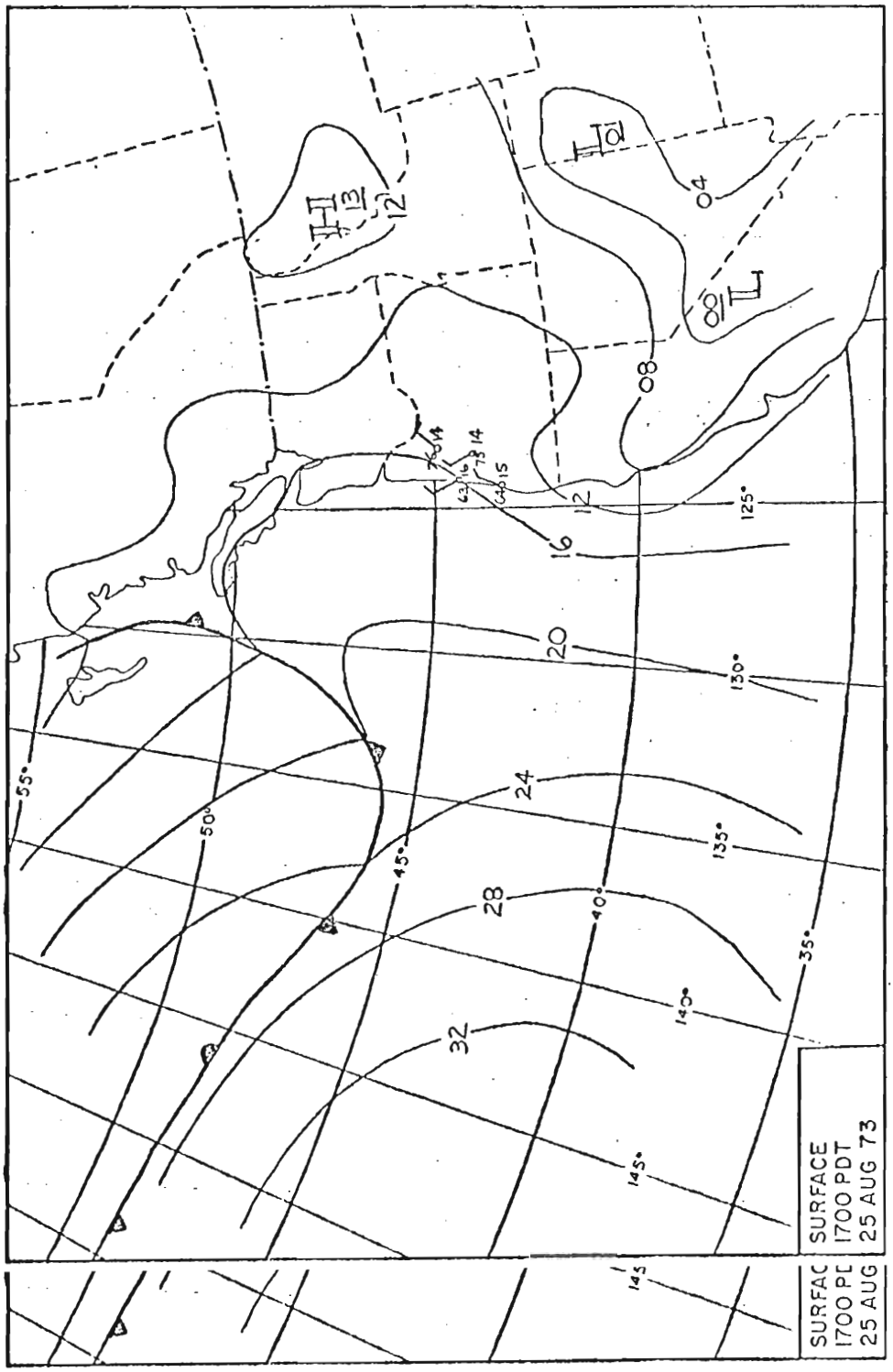

Fig. 5. Synoptic scale sea level pressure analysis for the Pacific coast area : area at 1700 PDT 25 Aug 1973.

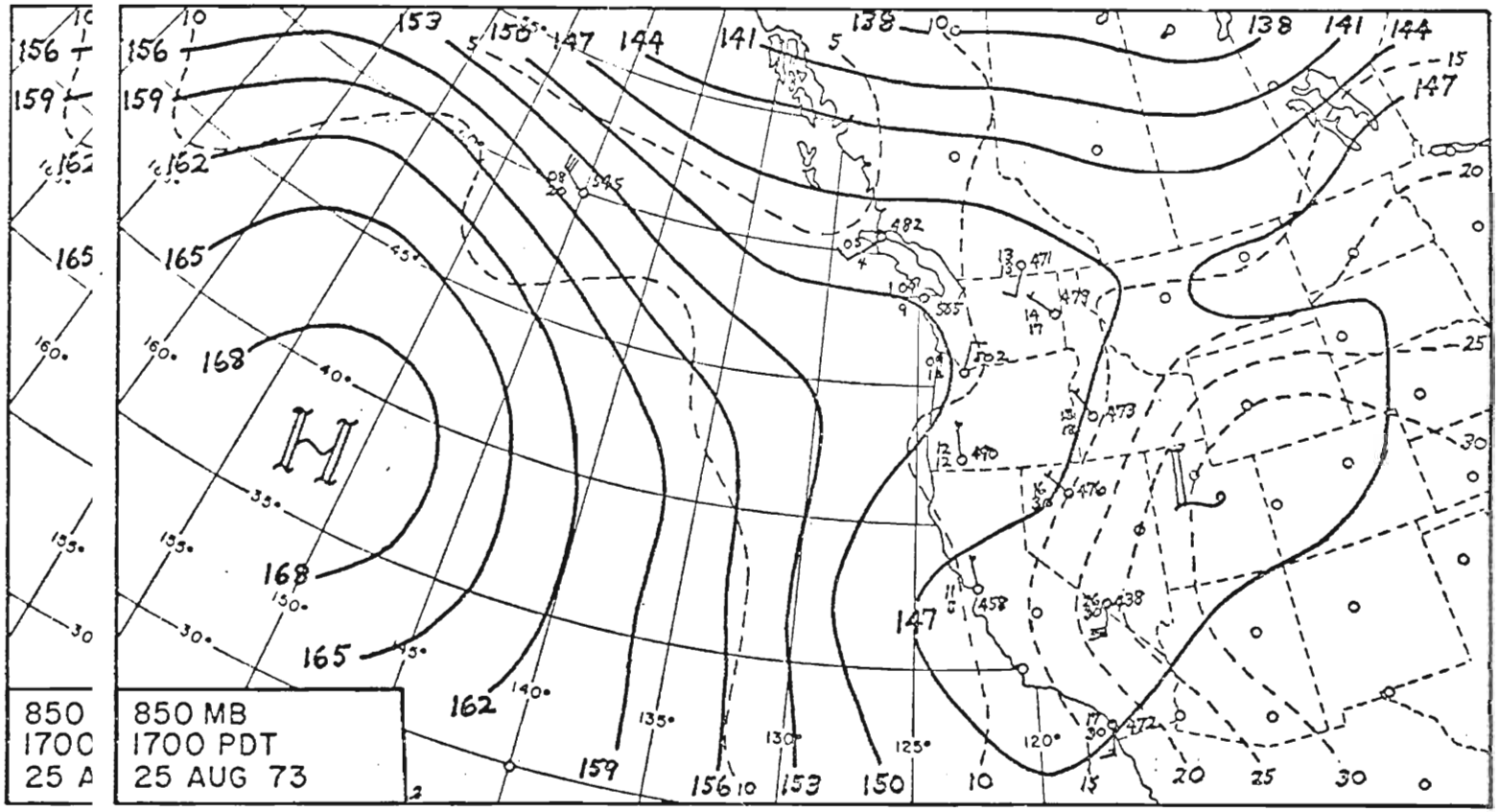

Fig. 6. 850-mb height contours (solid lines) and isotherms (dashed lines) for the 1 the Pacific coast area at 1700 PDT 25 Aug 1973.

upwelling event. Yet, there is no evidence of any synoptic scale feature which can be associated with the mesoscale offshore jet.

The mesoscale dew point temperature field is presented in Fig. 7. A distinct minimum appears at 10-15 km offshore, which corresponds approximately to the east side of the jet axis. The temperature field, which is not presented here, is much more constant with only 1.5C range over the study area. However, small increases in temperature are apparent where the sharpest dew pont drops occur, indicating evidence of subsidence where the relatively dry air is observed.

The width scale of this offshore jet is 20-30 km. Bunker (1965) observed a larger scale jet (order of 100 km) from approximately 100-200 km off the coast of Somalia, which is another coastal upwelling region. A speed maximum of 25 m sec^{-1} was observed for the Somalia jet.

From aircraft soundings, the vertical structure shows an inversion near 960 mb at 40 km seaward (D triangle). The inversion weakens at the coast and disappears inland. The dew point temperature vertical profile indicates a deeper well-mixed marine layer seaward.

Since the subsidence, with its associated jet, occurs as low as 152 m (500 ft) above the sea surface, one very important question arises. Is the jet and band of subsidence directly related to the sea surface temperature pattern? The sea surface temperature pattern for 25 August (Fig. 8) shows the isotherms generally aligned NE to SW, with coldest water near the coast in the southern half of the study area. A warm band of water extends from the NE corner to the SW part of the study area.

water near the coast in the southern half of the study area. A warm band of water extends from the NE corner to the SW part of the study area.
Since strong southerly winds occurred on 23 and 24 August, the sea surface temperatures on 25 August are warmer than normal. Holladay and O'Brien

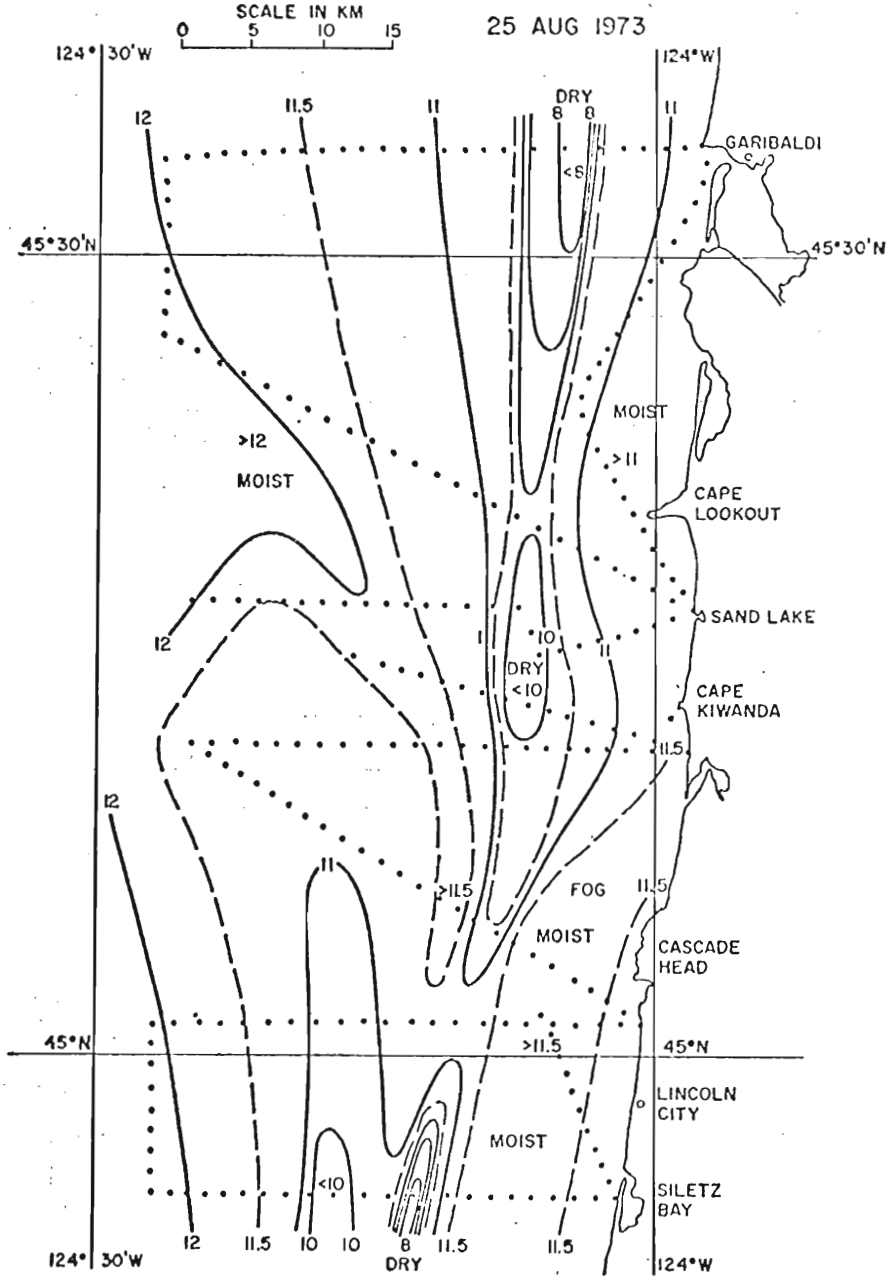

Fig. 7. Dew point temperature (°C) at 152 m (500 ft) for the period 1300-1500 PDT 25 Aug 1973.

Fig. 7. Dew point temperature (°C) at 152 m (500 ft) for the period 1300-1500 PDT 25 Aug 1973.

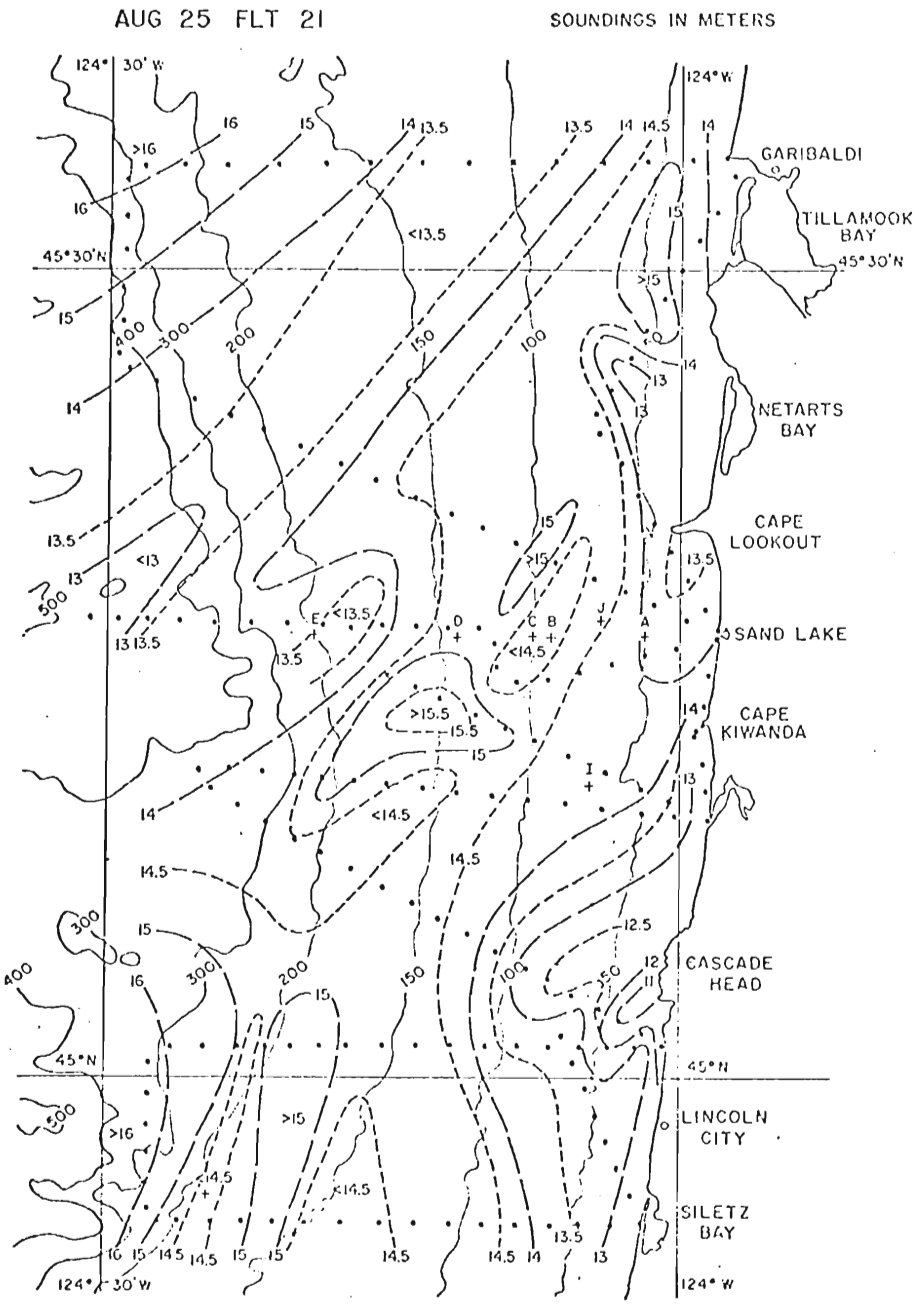

Fig. 8. Sea surface temperatures (°C) for the period 1300-1500 PDT 25 Aug 1973. The ocean bottom topography is represented by the solid lines, with depths in m.

(1974) discuss the mesoscale variability of sea surface temperatures during CUE II. In the following sections, the sea surface temperature pattern for other cases will be examined and compared with the 25 August pattern in an effort to determine if there is a direct relation between the sea surface temperature pattern and the occurrence of an offshore wind speed maximum.

b. Case of 18 August

During the early afternoon on 18 August, the NCAR aircraft made a special flight seaward. After making routine soundings at A (triangle) and C (triangle), the aircraft headed north to the Sand Lake buoy line. Beginning at the coast at 152 m (500 ft), the aircraft flew 132 km seaward, then ascended to 1524 m (5000 ft) and descended back to 152 m (500 ft). Thereafter it followed the same path along the buoy line back to Sand Lake. The purpose of this flight was to examine the change in sea surface temperatures, winds, and other parameters seaward from the coastal upwelling zone.

The synoptic scale pattern for 1700 PDT 18 August is similar to that of 25 August. At the surface, a large anticyclone is centered near 145W, 50N. Coastal pressure gradients are about the same on both days, but the thermal gradient is slightly stronger on 18 August, apparently due to lower sea surface temperatures at the coast.

As on 25 August, a distinct wind speed maximum (Fig. 9, top) appears from 15-30 km seaward on both the outbound and inbound flight. The total time between leaving the coast and returning is about 1.5 hours. During

time between leaving the coast and returning is about 1.5 hours. During

this time, the total wind speed has increased everywhere by 1-2 m sec^{-1}, but the wind speed maximum is evident on both outbound and inbound flights. Seaward, the wind speeds decrease and become more constant. During the

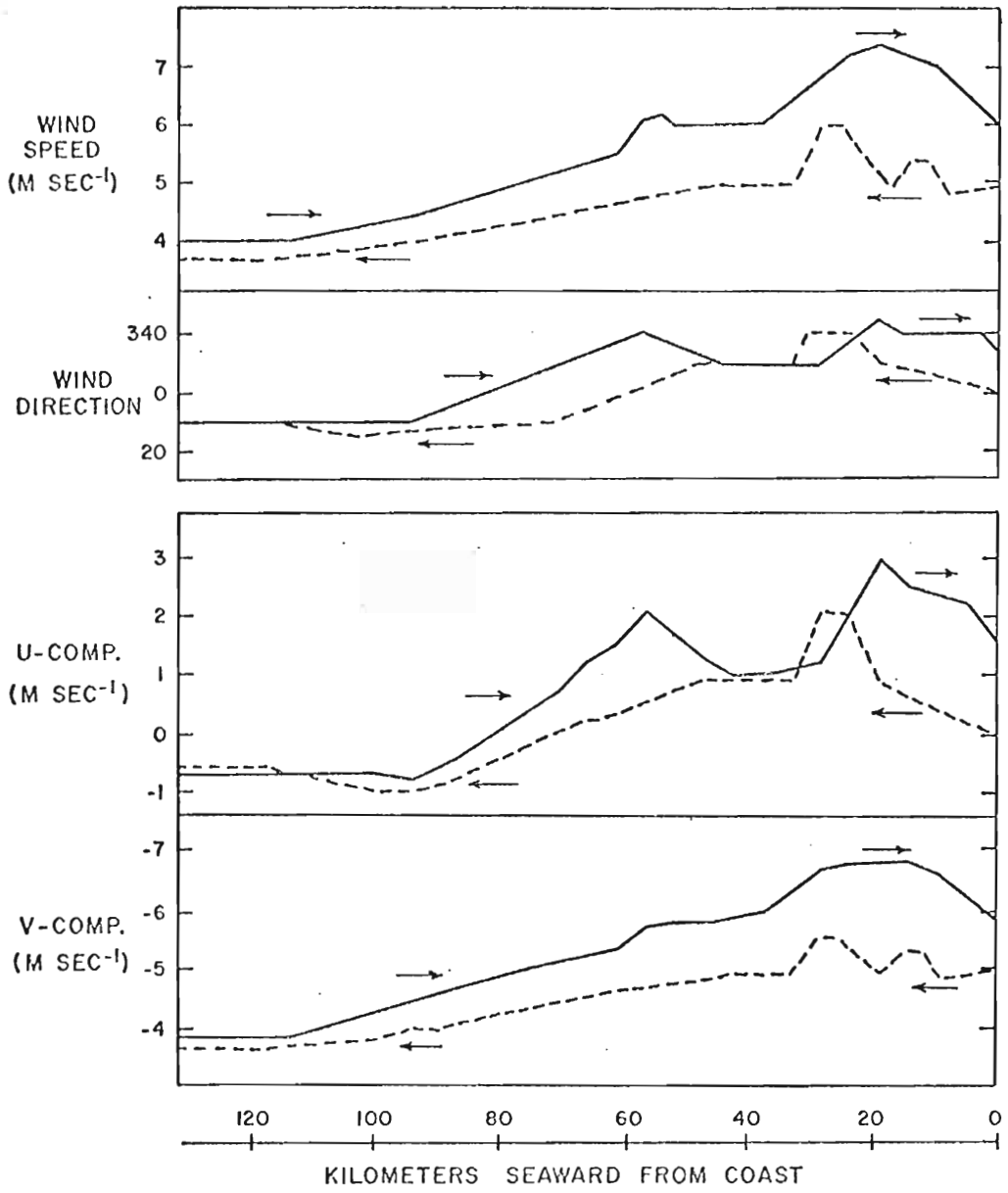

Fig. 9. Profiles of wind speed, direction, and u, v components at 152 m (500 ft) above the sea surface from the coast to 132 km seaward for 18 Aug 1973. Dashed lines represent data along the outbound flight (1420-1448 PDT) and solid lines along the inbound flight (1507-1535 PDT).

components at 152 m (500 ft) above the sea surface from the coast to 132 km seaward for 18 Aug 1973. Dashed lines represent data along the outbound flight (1420-1448 PDT) and solid lines along the inbound flight (1507-1535 PDT).

inbound flight, a secondary maximum appears to be forming 50-60 km seaward and the area occupied by the primary maximum appears to have widened. Consistent with the 25 August observations, the wind direction is more westerly in areas of wind speed maximum. From the u and v components (Fig. 9), it is apparent that the largest variations in the east-west plane occur in the u component.

Associated with the low level jet is evidence of subsidence (Fig. 10), as shown by the dramatic drop in dew point temperature and slight increase in air temperature. On the earlier (outbound) flight, the subsidence region lies slightly east of the jet, as in the 25 August case. On the return (inbound) trip, the area of subsidence has broadened out and the primary jet axis appears to lie within the area of subsidence. Even though the jet appears to have shifted, the area of subsidence has not propagated toward the coast. One possible explanation is the orographic effect of the coastal mountains, preventing the subsidence from moving any closer than about 10 km offshore. The relative humidity even increases in time within the nearest 10 km of the coast, probably due to the increased westerly component which leads to an increase of the topographically-induced upward motion.

The sea surface temperature (Fig. 10) ranges from 8C at the coast to 15C seaward. The largest gradient is within 10 km of the coast. The reason that the nearshore sea surface temperatures are 3^{o}-5^{o} colder on 18 August than on 25 August is due to several days of sustained northerlies previous to 18 August.

August than on 25 August is due to several days of sustained northerlies previous to 18 August.

The vertical temperature profiles (Fig. 11) show that the greatest stability is found in the lowest 50 mb over the coastal upwelling region near the coast. Unstable lapse rates occur seaward in the lowest layers.

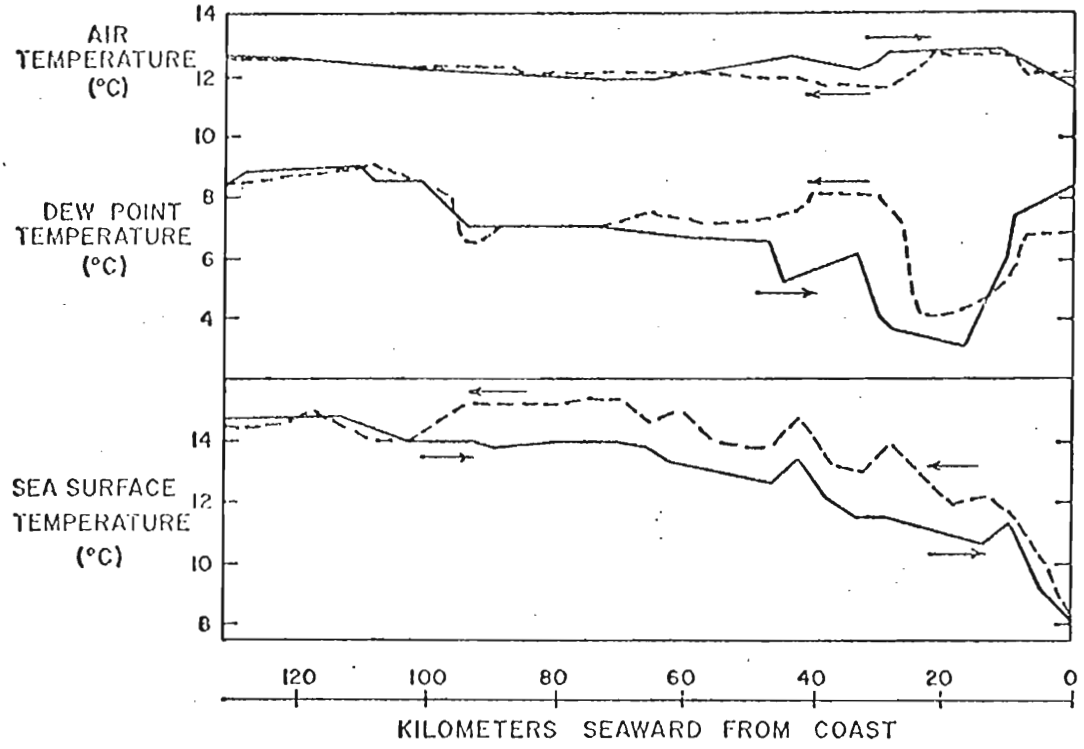

Fig. 10. Same as Fig. 9 except for air temperature, dew point temperature, and sea surface temperature for 18 Aug 1973.

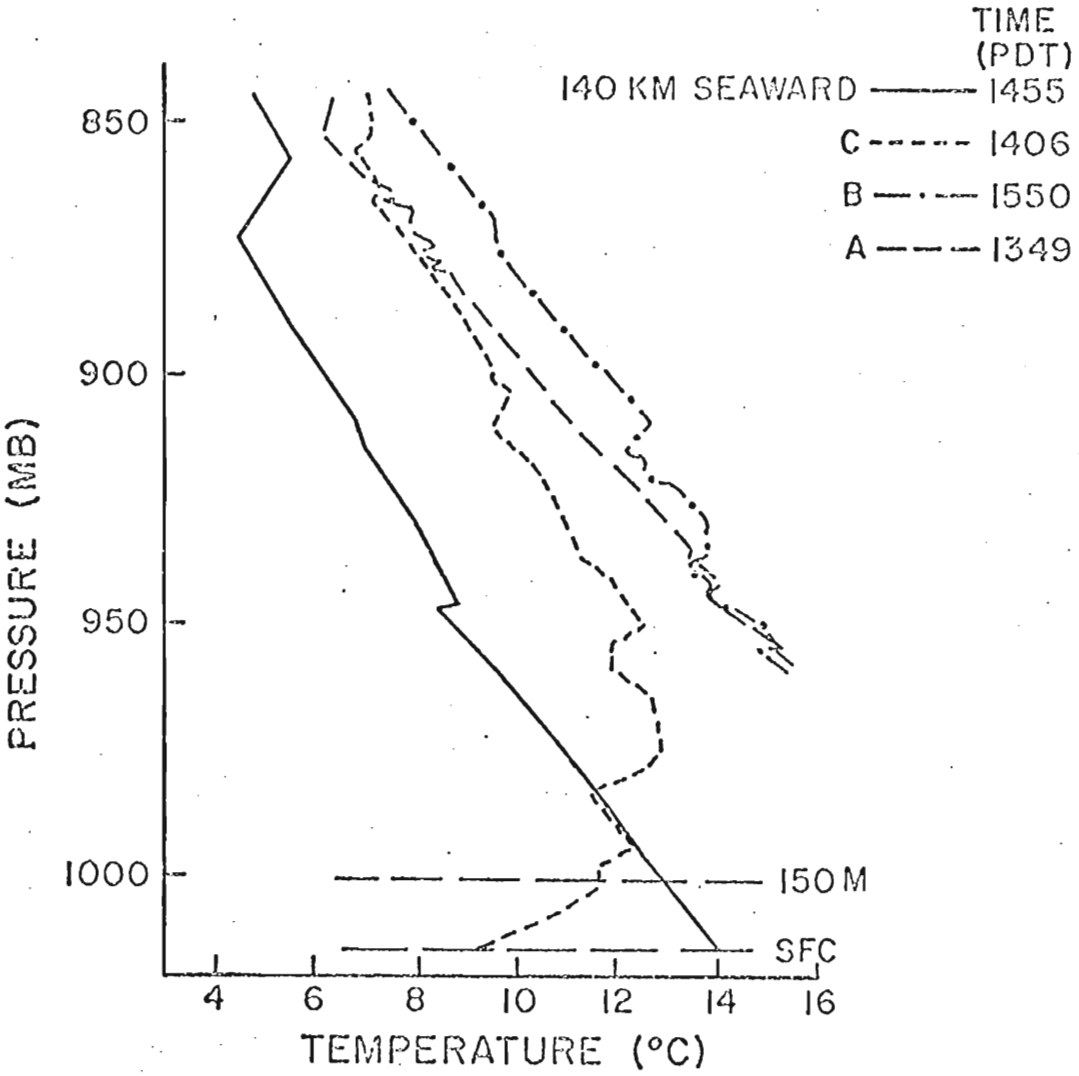

Fig. 11. Profiles of temperature vs. pressure for the four aircraft soundings on 18 Aug 1973. The time (PDT) listed for each sounding is the time at the beginning of each descent. Refer to Figs. 1 and 2 for the relative locations of soundings A, B, and C and the approximate height at the beginning and end of each descent. For the lowest 150 m, the temperature has been linear interpolated down to the estimated temperature at the sea surface.

at the sea surface.

During the morning of 18 August, the aircraft flew a regular Type I pattern (Fig. 1). A well-defined jet axis (Fig. 12) is apparent from 10-20 km offshore, associated with a sharp dew point gradient (Fig. 13). However, unlike the afternoon pattern, the drier air extends onshore. Near the coast, the 152 m (500 ft) winds have a slight easterly component. The 0830 PDT pibal winds for Cape Kiwanda show predominately north-easterly winds up to 2700 m. The wind speed increases with height up to 500 m and then decreases. The northerly component was observed to be 10.3 m sec^{-1} at 500 m, and the easterly component 4.5 m sec^{-1}. Thus, during the morning, it seems likely that subsidence is enhanced by downslope winds at the coast.

As the thermal gradient between land and sea intensifies, the sea breeze develops and, because of increased upslope winds, wipes out the subsidence within the nearest 10 km of the coast. Pibal data verifies this, indicating a speed maximum at 200 m and a slight westerly component up to 500 m. Yet, a band of subsidence persists offshore. This is the apparent source of momentum for the offshore low level jet.

c. Case of 14 August

On the synoptic scale pattern, the only major difference from the 25 August case is the extension of the thermal low, which results in intense heating inland. Thus, the thermal gradient is much stronger during the afternoon on 14 August than on our previous case studies. As a result, surface wind speeds are greater, reaching a maximum of 10 m sec^{-1} by 1800 PDT.

1800 PDT.

A sharp marine inversion (Fig. 14) occurs near 950 mb. The 152 m (500 ft) dew point temperature and temperature fields are very homogeneous (varying less than 1C) over the entire study area and, therefore, not

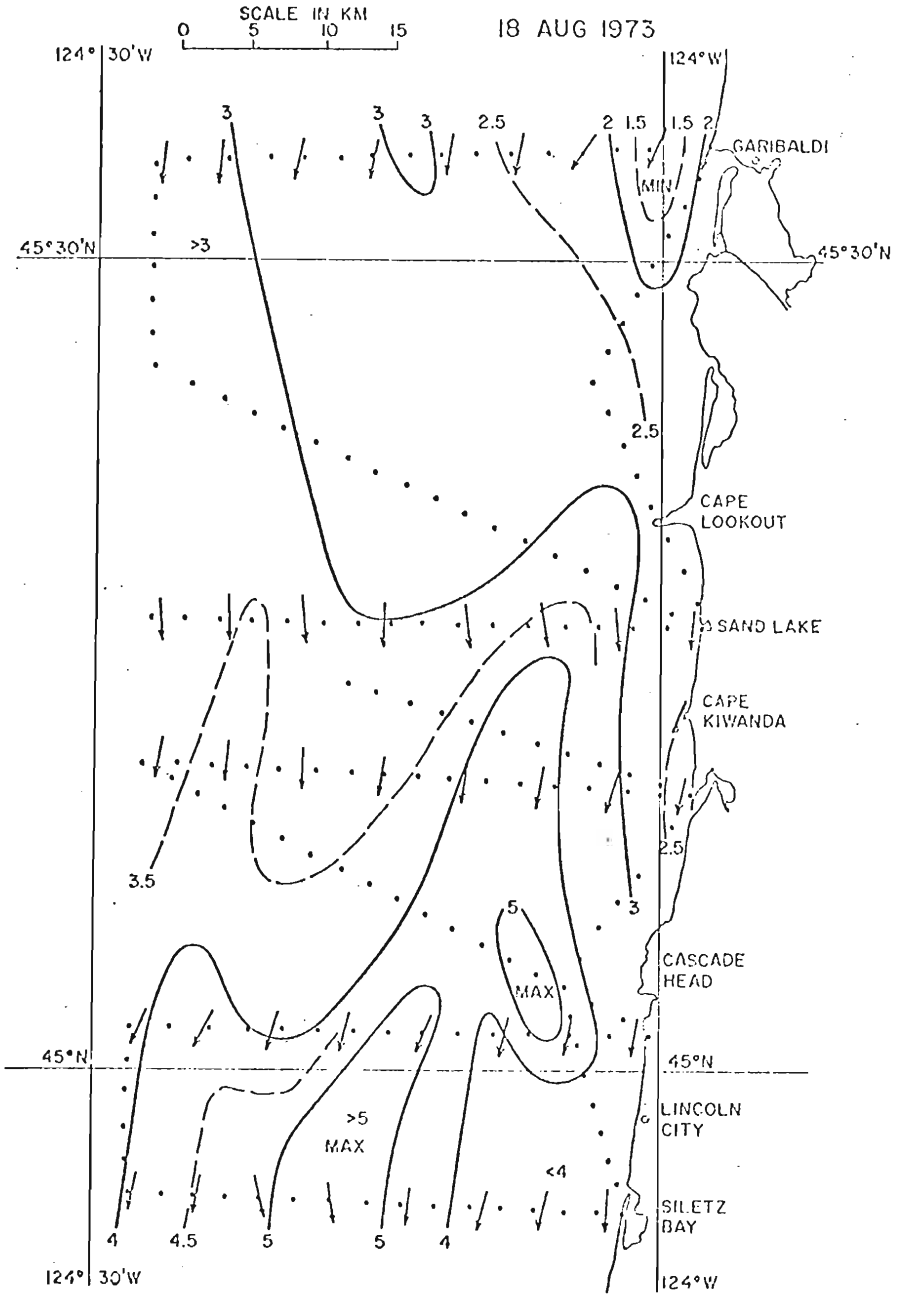

Fig. 12. Isotachs of wind speed (m sec^{-1}) at 152 m (500 ft) for the period 0930-1130 PDT 18 Aug

Fig. 12. Isotachs of wind speed (m sec^{-1}) at 152 m (500 ft) for the period 0930-1130 PDT 18 Aug 1973. Vectors show direction of winds. Dotted lines show the aircraft flight pattern.

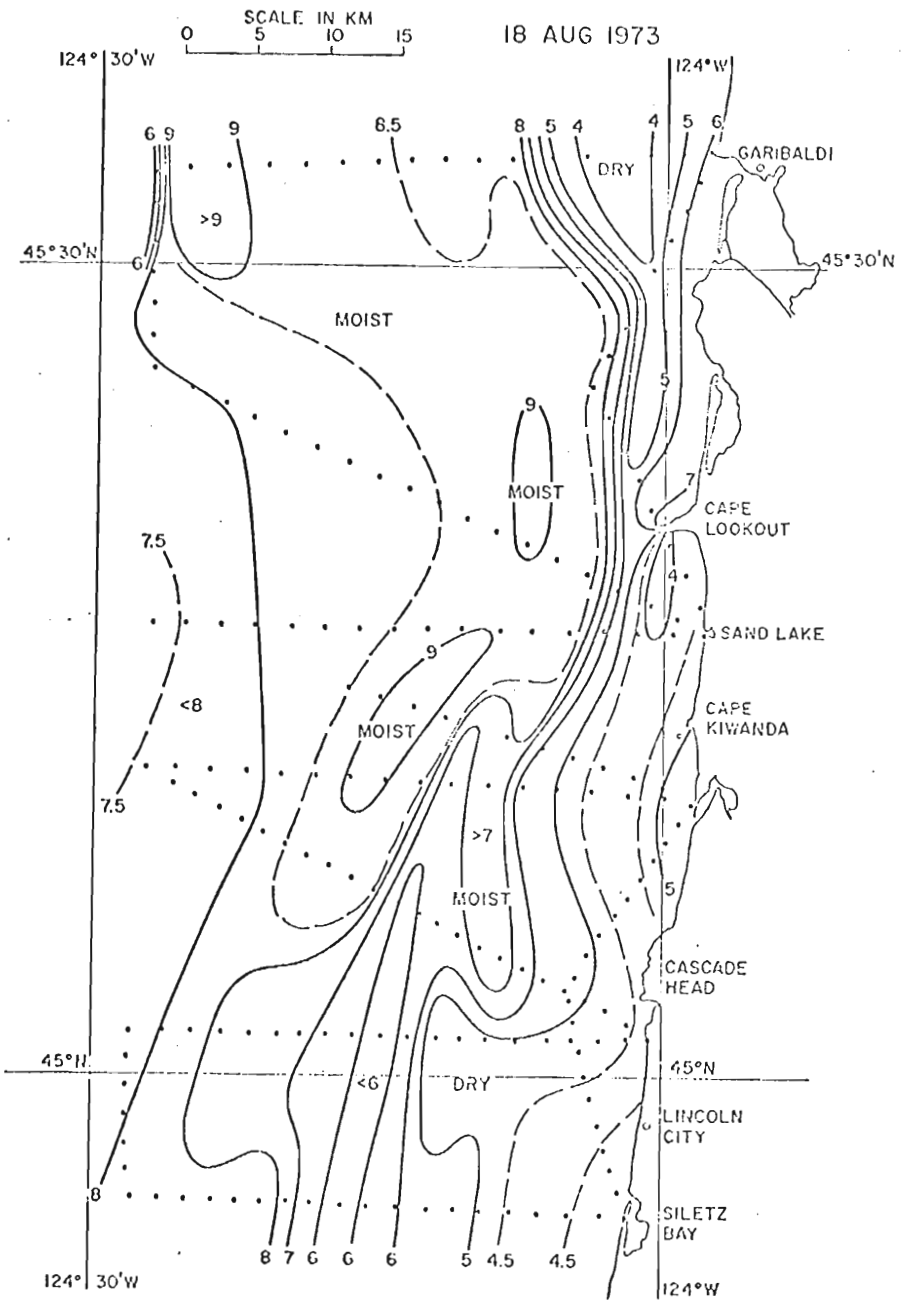

Fig. 13. Dew point temperatures (°C) at 152 m (500 ft) for the period 0930-1130 PDT 18 Aug 1973.

Fig. 13. Dew point temperatures (°C) at 152 m (500 ft) for the period 0930-1130 PDT 18 Aug 1973.

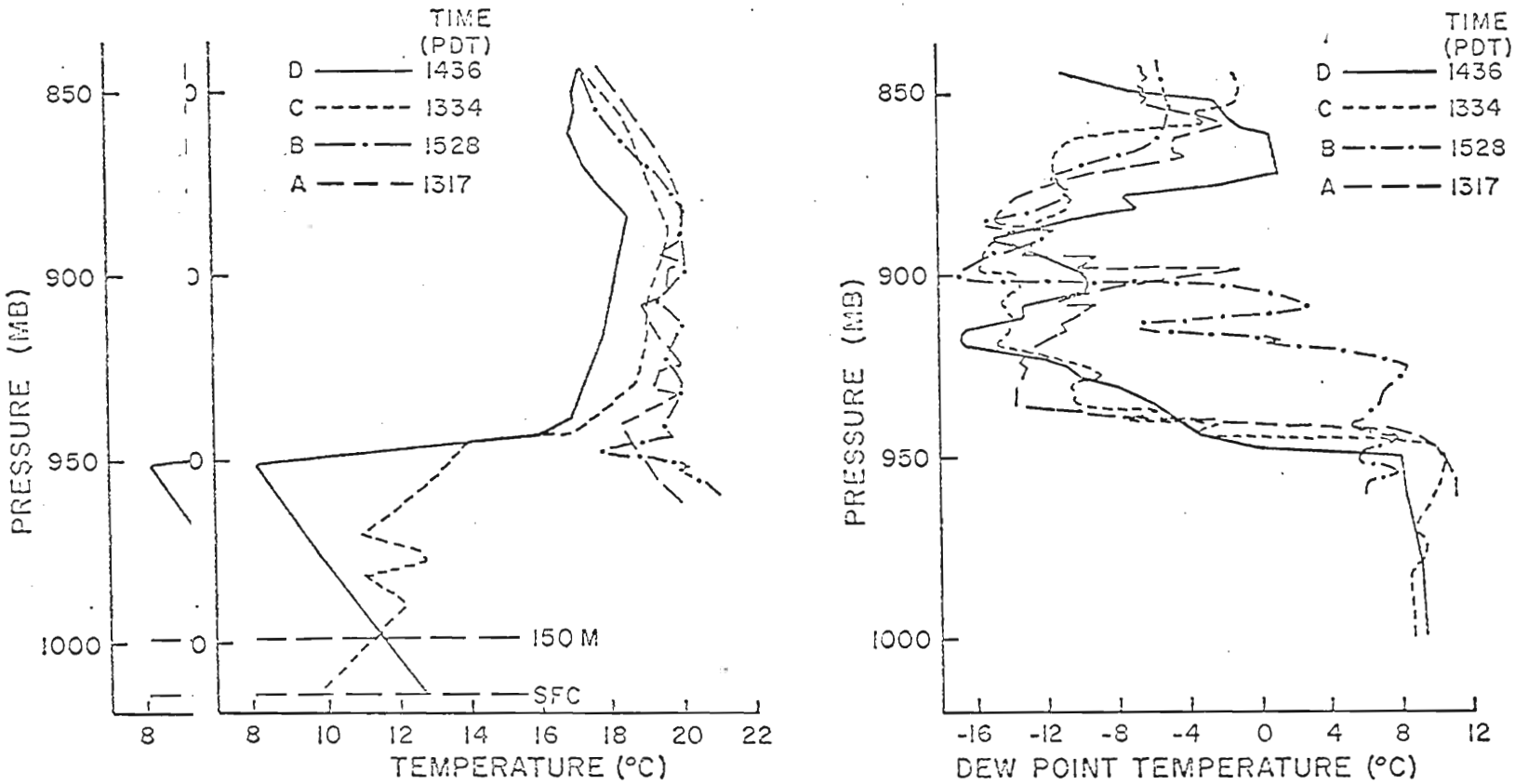

Fig. 14. Profiles of temperature (left) and dew point temperature (right) vs. pressure for aircraft soundings on 14 Aug 1973. The time (PDT) listed for each sounding is the time at the beginning of each descent. Refer to Figs. 1 and 2 for the relative locations of the soundings and the approximate height at the beginning and end of each descent. For the lowest 150 m, the temperature has been linear interpolated down to the estimated temperature at the sea surface.

analyzed. The winds (Figs. 15 and 16) are strongest near the coast and decrease seaward.

Sea surface temperatures (Fig. 17) are very cold near the coast and increase rapidly seaward. The effect of the colder, coastal water on the stability can be seen by comparing the two temperature soundings in Fig. 14. The coastal wind speed maximum is located over the region of coldest sea surface temperatures. This suggests that the coastal thermal gradient is the primary mechanism producing the speed maximum. Unlike the offshore speed maximum of 18 and 25 August, the coastal speed maximum here is not associated with a region of subsidence. Thus, we conclude that the low level jet has a structure (or existence) which depends on the basic stratification and depth of the marine layer. When the marine inversion is well developed, the subsidence does not penetrate to the extent required to provide the momentum necessary for the offshore low level jet.

d. Summary of other Type I flight cases

In six other cases examined, with moderate to strong northerlies, no offshore jets were observed. The sea surface temperatures were generally coldest near the coast, with strongest gradients mainly within the nearest 20 km of the coast, on days with no offshore wind speed maximum.

As noted in the previous case studies, horizontal temperature gradients at or above the 150 m level do not necessarily have the same sign as sea surface temperature gradients (see Figs. 10, 11, and 14). We found this to be true, also, for other cases examined. The horizontal dew point temperature fields were, for the most part, very uniform, with no sharp gradients. Apparently, if low level subsidence did occur on

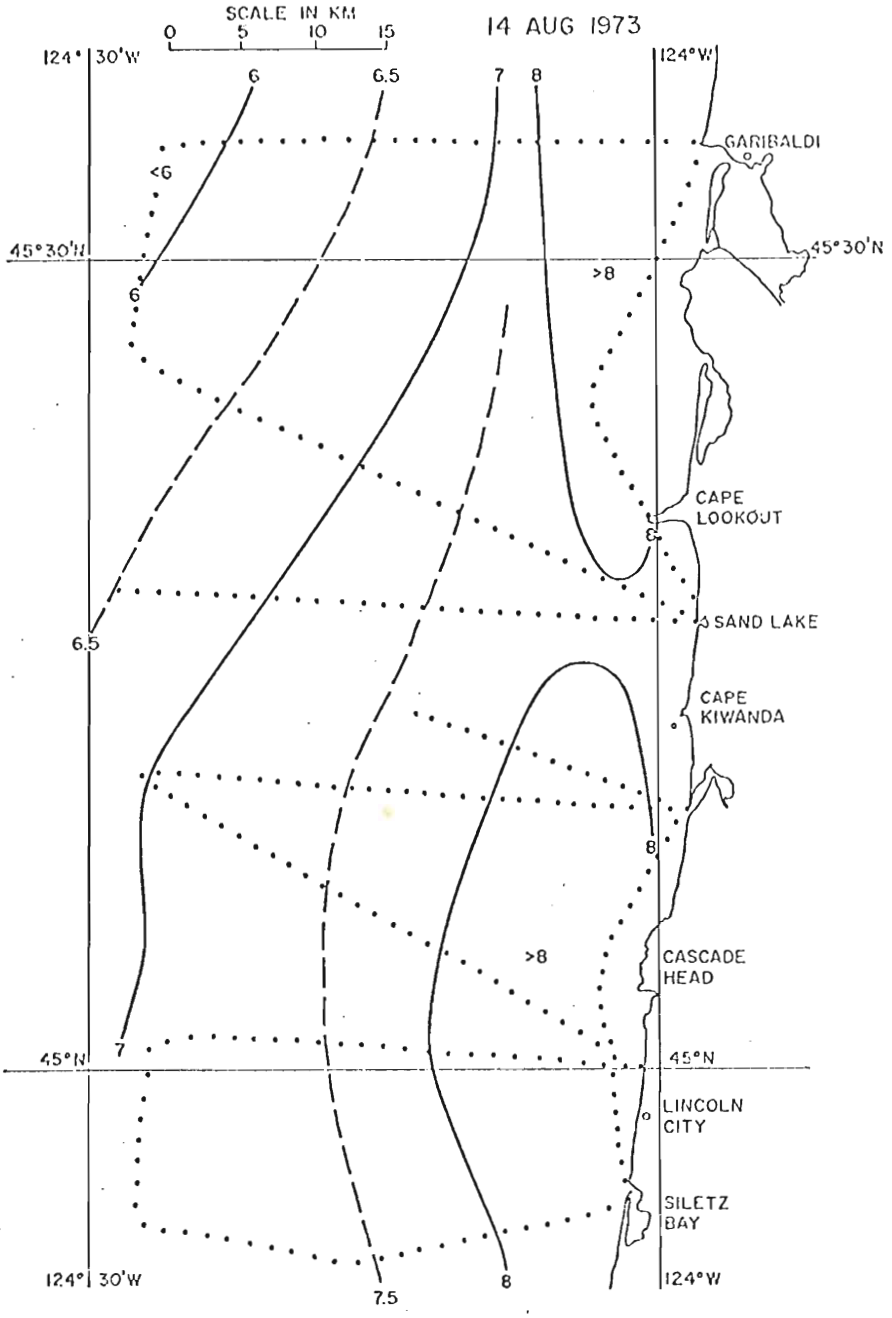

Fig. 15. Isotachs of wind speed (m sec^{-1}) at 152 m (500 ft) for the period 1330-1530 PDT 14 Aug 1973.

Fig. 15. Isotachs of wind speed (m sec^{-1}) at 152 m (500 ft) for the period 1330-1530 PDT 14 Aug 1973.

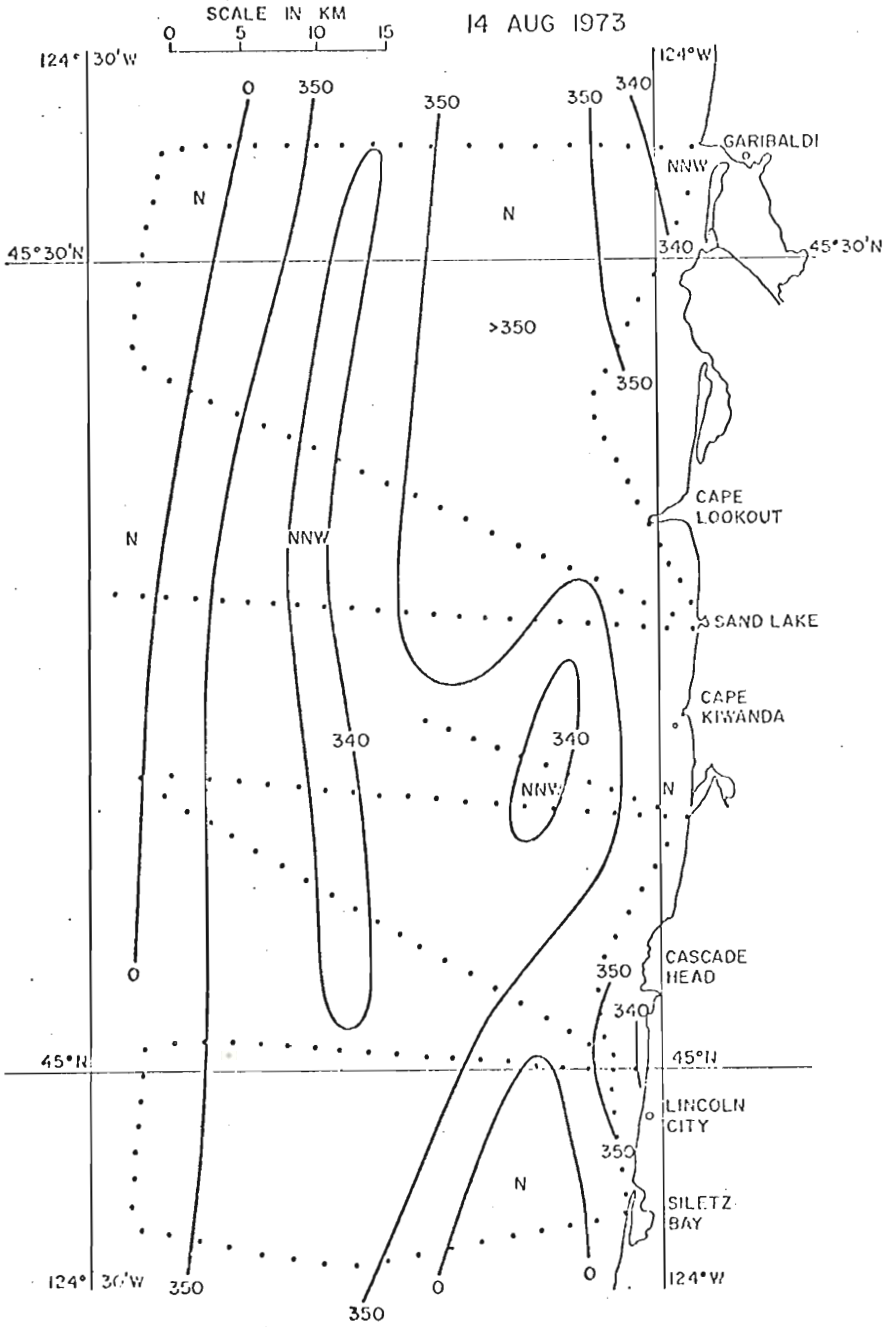

Fig. 16. Isogons of wind direction at 152 m (500 ft) for the period 1330-1530 PDT 14 Aug 1973.

Fig. 16. Isogons of wind direction at 152 m (500 ft) for the period 1330-1530 PDT 14 Aug 1973.

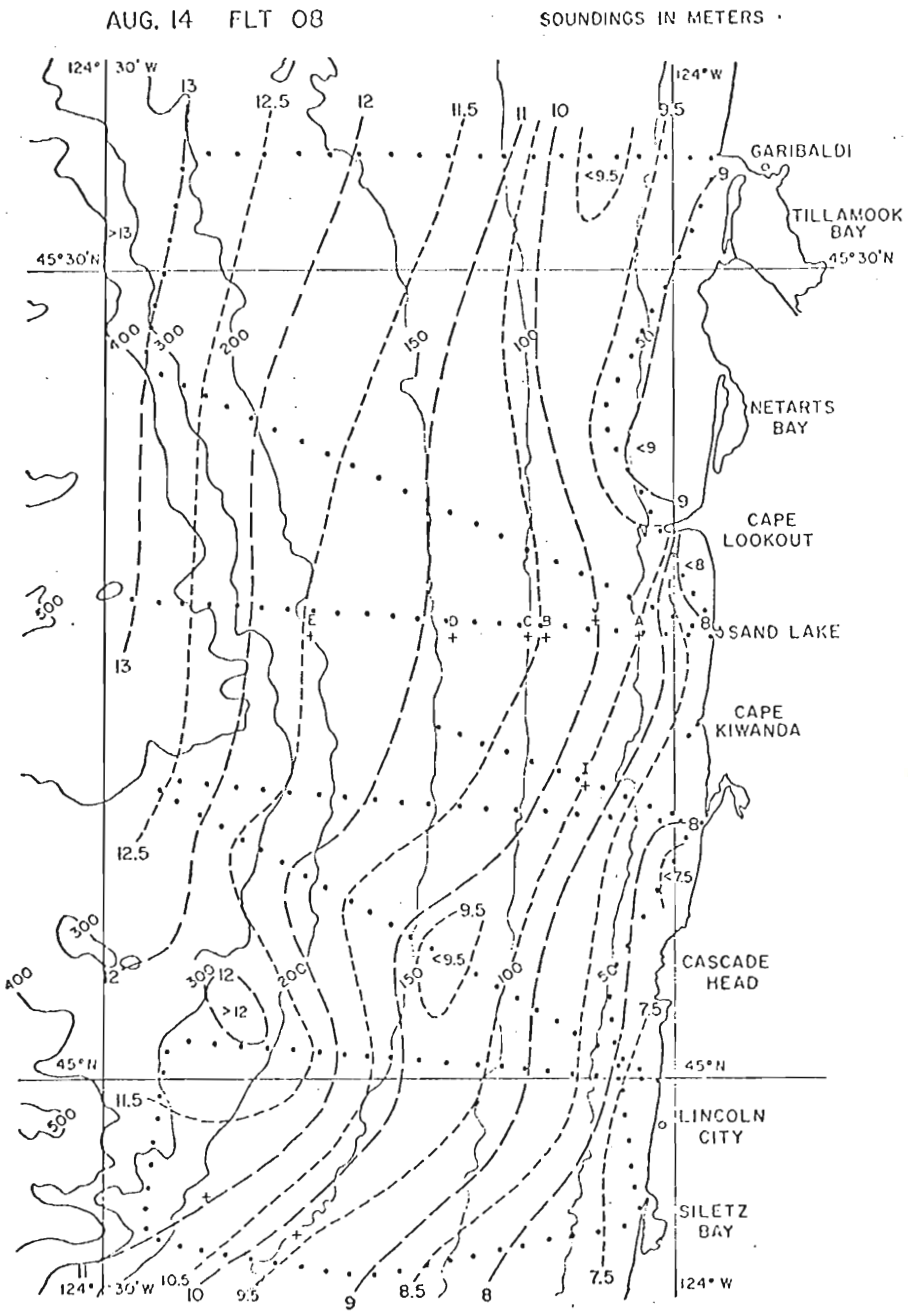

Fig. 17. Sea surface temperatures (°C) for the period 1330-1530 PDT 14 Aug 1973. The ocean topography is represented by the solid lines, with depths

Fig. 17. Sea surface temperatures (°C) for the period 1330-1530 PDT 14 Aug 1973. The ocean topography is represented by the solid lines, with depths in m.

these days, it remained above the 152 m (500 ft) level. In the following section, we shall examine vertical cross sections of the moisture field and find that the subsidence region does, indeed, generally remain above 152 m (500 ft) level and is strongest over the upwelling zone.

4. THE VERTICAL STRUCTURE OF THE MOISTURE, TEMPERATURE, AND WIND

In this section we present vertical cross sections of the mixing ratio and temperature, analyzed from Type II flight data (Fig. 2). Three different cases are considered: (1) a case without an inversion and with a deep marine layer over the ocean; (2) a case without an inversion and with a shallow marine layer over the ocean; (3) a case with a sharp, low level marine inversion. By "without an inversion", we mean no significant inversion in the lowest 1500 meters over the ocean. By "marine layer over the ocean", we mean the lower, relatively moist layer extending up to where a sharp gradient in the mixing ratio occurs. Typically, we found this to be about 6-7 g kg^{-1} for the cases presented here. In addition, horizontal wind vectors along each flight level are presented for the case of 26 August and discussed for all three cases.

a. Case of 26 August

The synoptic scale pattern for 1700 PDT 26 August shows a weak surface front 200-300 km east of the central Oregon coast. This is the same frontal system which is seen over the Pacific on 25 August (Fig. 5). The front appeared to have very little effect on the coastal pressure pattern and weather. Some light rain showers occurred offshore; however, during the frontal passage (around 1300 PDT according to synoptic charts), the Newport jetty winds showed no change in direction as winds remained

the Newport jetty winds showed no change in direction as winds remained NNW. From 1100-1300 PDT, a 3 m sec^{-1} increase in wind speed was observed, but this increase is probably due to diurnal effects; coastal wind speeds

typically increase from morning to afternoon, as a result of differential heating. After the frontal passage, the sea level pressure pattern and wind field appeared almost unchanged. Thus, in spite of a weak frontal passage, we feel this case is suitable for studying the mesoscale meteorology over an upwelling region.

The cross section of temperature for 26 August (Fig. 18) shows no significant inversions for the lowest 1500 m, except for an inversion base seaward near the 1500 m level. In the cross section of mixing ratio (Fig. 19), a broad tongue of relatively dry air is observed over the coastal region. Seaward the marine layer deepens considerably.

The mesoscale wind field (Fig. 20) for late afternoon, 26 August, is quite interesting. Note the pronounced horizontal difluence directly above the coast on almost every flight leg. Even though there is no low level inversion, the winds lying offshore have a slight easterly component between 500 and 1200 m, while the winds lying onshore have a westerly component at every level. Although the aircraft made no measurements on vertical velocity, the combination of drier air in the moisture field and horizontal difluence in the wind field substantially support evidence of subsidence.

The sea breeze circulation from the coast inland is apparent from aircraft and pibal winds. The return flow of the sea breeze circulation appears as a minimum in the westerly component at approximately 1300-1500 m, where the westerlies diminish considerably. Pibal winds show the westerly component again above 1500 m. By this time of day (1600-1800 PDT),

1500 m, where the westerlies diminish considerably. Pibal winds show the westerly component again above 1500 m. By this time of day (1600-1800 PDT), the sea breeze circulation is usually well developed and extends eastward into Willamette Valley (50 km inland) as is the case here. Johnson and

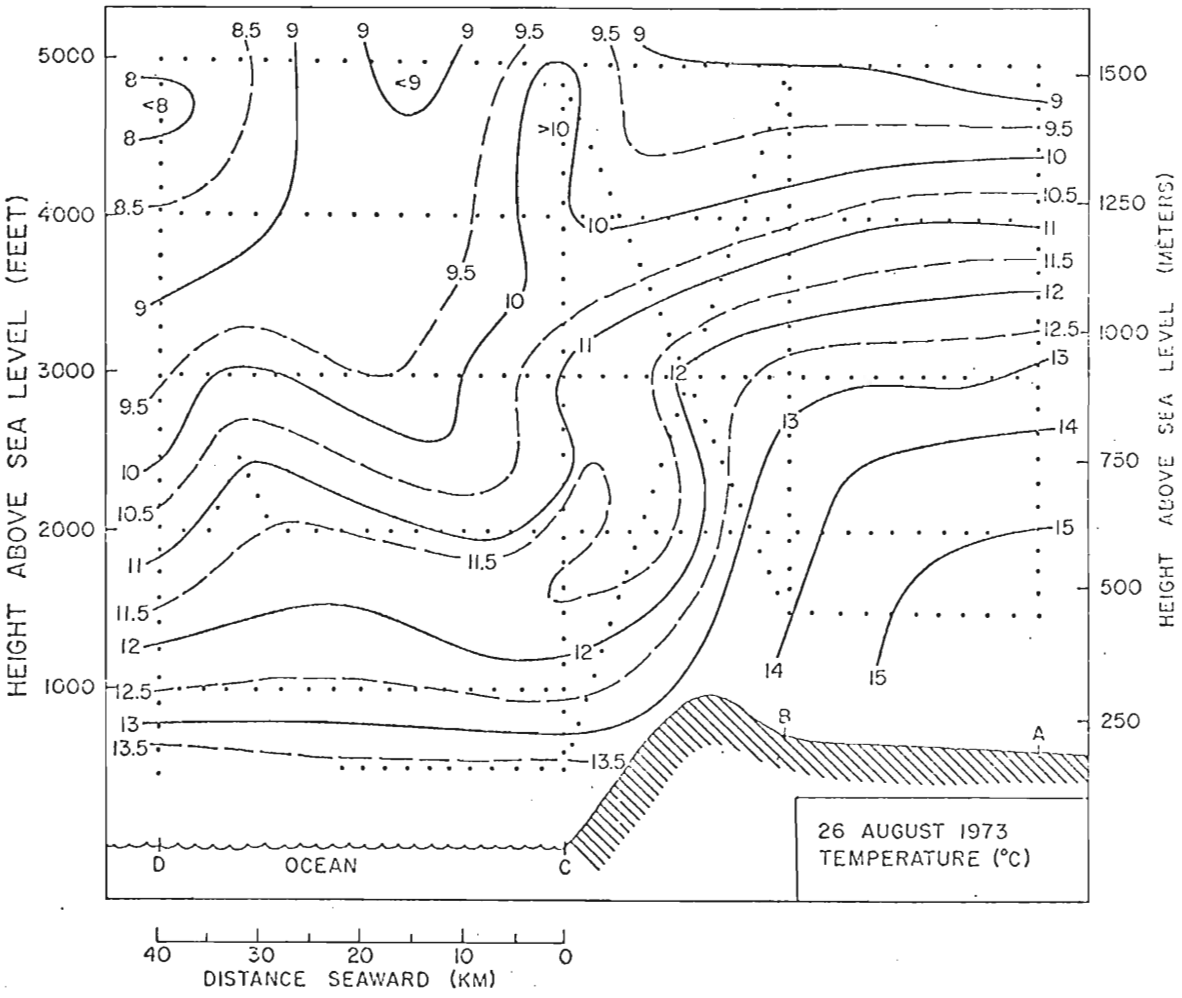

Fig. 18. Temperature cross section for the period 1600-1830 PDT 26 Aug 1973.

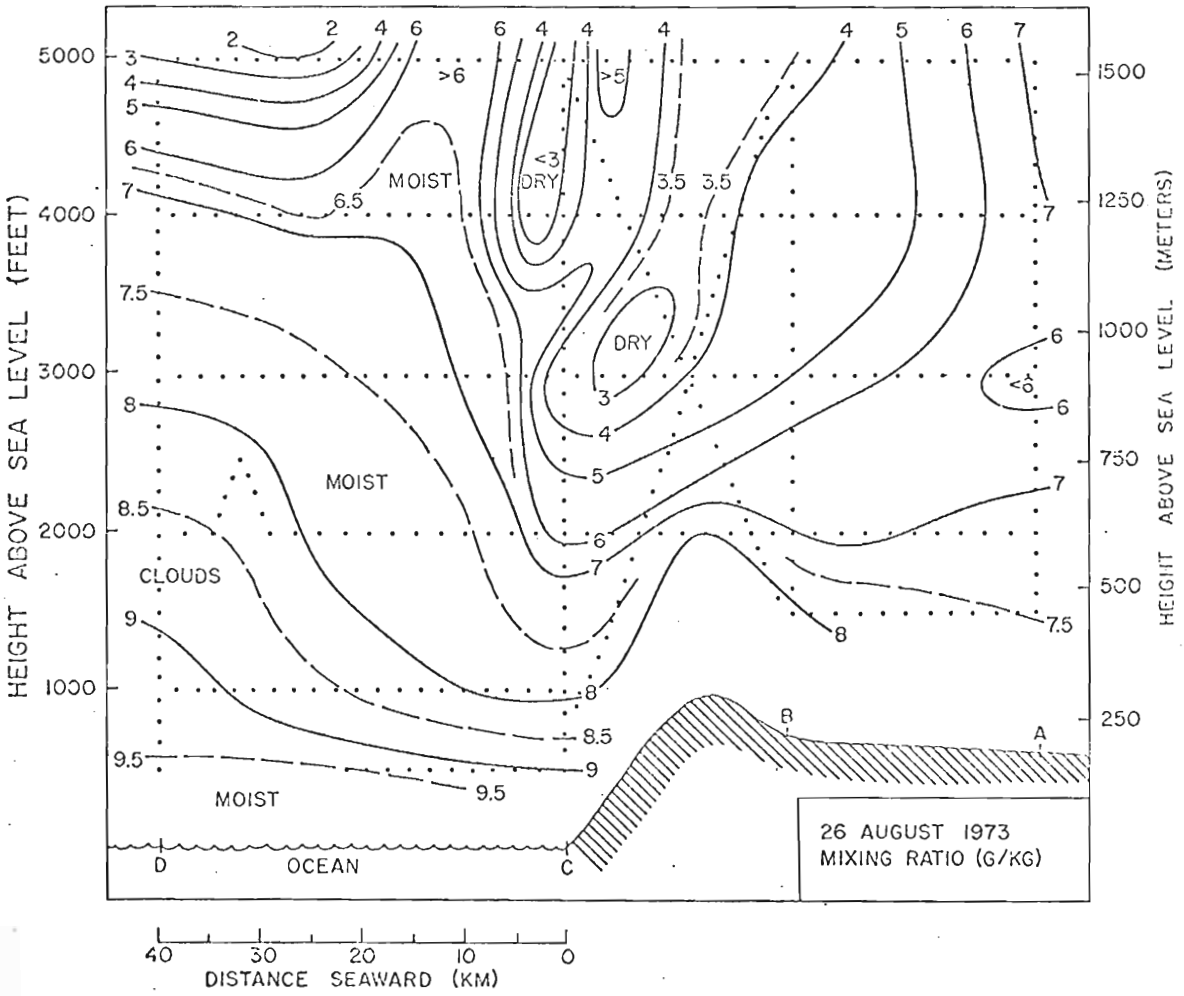

Fig. 19. Cross section of mixing ratio (g kg^{-1}) for the period 1600-1830 PDT 26 Aug 1973.

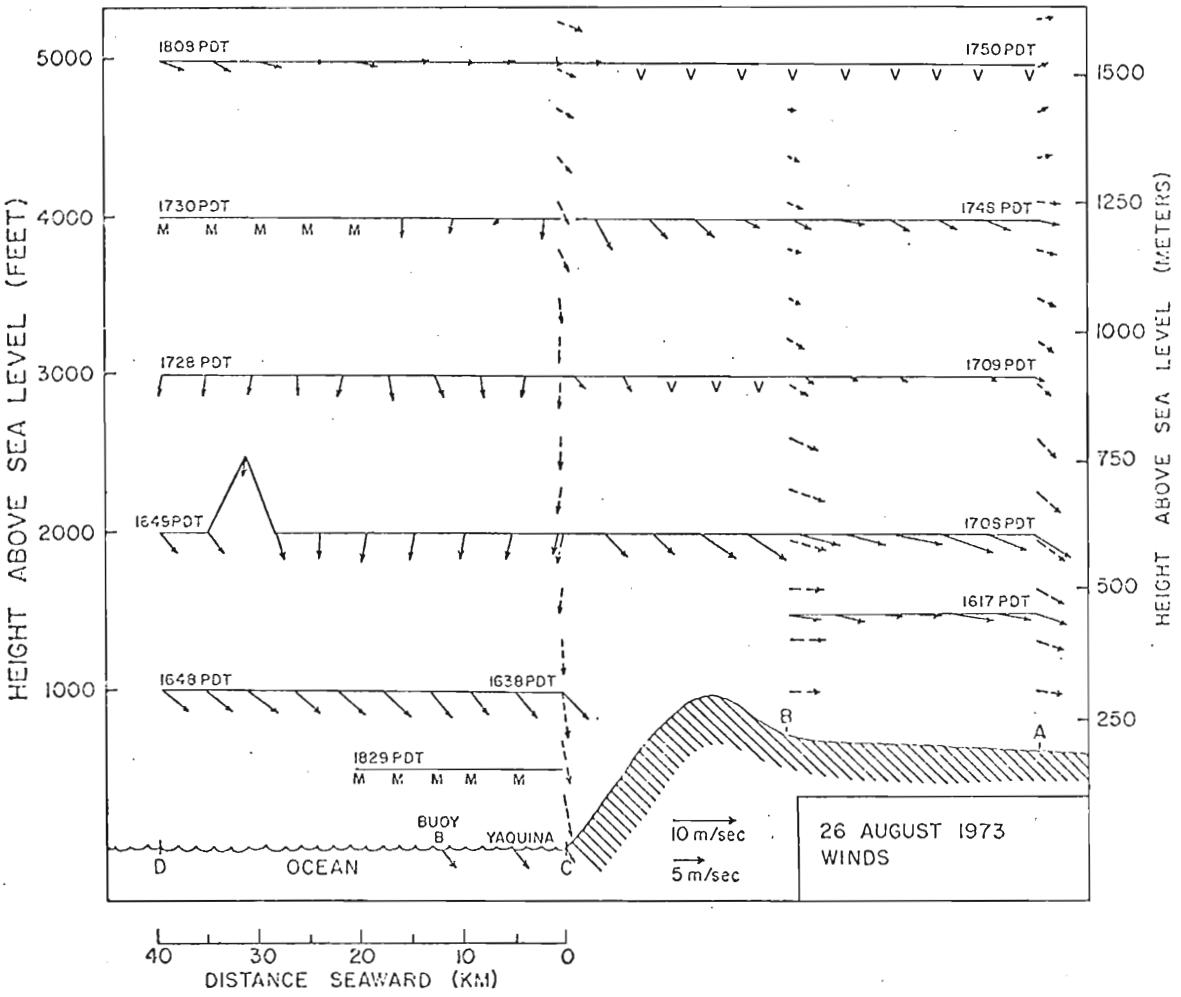

Fig. 20. Solid vectors represent horizontal winds measured by the NCAR aircraft, utilizing a Doppler navigation system. Time (PDT) is indicated along each flight leg. Dashed vectors represent pibal (or rawinsonde) winds for either 1615 PDT or 1815 PDT, whichever is closest to the aircraft flight time. M designates Doppler in memory; V, light and variable winds. Wind vectors relate to scale at lower right. In addition, three surface observations are plotted.

surface observations are plotted.

O'Brien (1973) have described the nature of the sea breeze circulation for the central Oregon coast region for a similar period during 1972. With the return flow of the sea breeze circulation aloft and the strong westerly component of flow in the lower levels over land, it is suggested that the presumed subsidence over the coastal region is associated with the west end of the sea breeze circulation.

From 0630 PDT to 1030 PDT 26 August, vertical profiles of wind speed at Cape Kiwanda show an increase of wind speed with height from the surface up to 500-700 m, where the maximum is 6-7 m sec^{-1}. From 1215 PDT to 1817 PDT, wind speeds are greatest in these lowest 300 m and decrease with height. After 2030 PDT, the vertical profiles of wind speed resemble that of the morning. This suggests that higher momentum aloft is transferred downward with the onset of the sea breeze, increasing the coastal subsidence. Johnson and O'Brien (1973) found similar vertical profiles in the mean for August 1972 for morning vs. afternoon cases.

b. Case of 27 August

Here we present a case where the subsidence did, indeed, extend almost down to the sea surface during the late afternoon (Fig. 21). Notice that the seaward marine layer has lowered by approximately 600 m from 26 August to 27 August. Apparently, large scale subsidence aloft has increased.

The synoptic scale pattern for 27 August is similar to previous cases. An extension of the Pacific High inland at the surface and the strengthening of the westerly flow aloft act to reduce the coastal pressure and thermal gradients. Northerly winds, although not as strong as in previous cases, were observed to reach 5 m sec^{-1} during the afternoon.

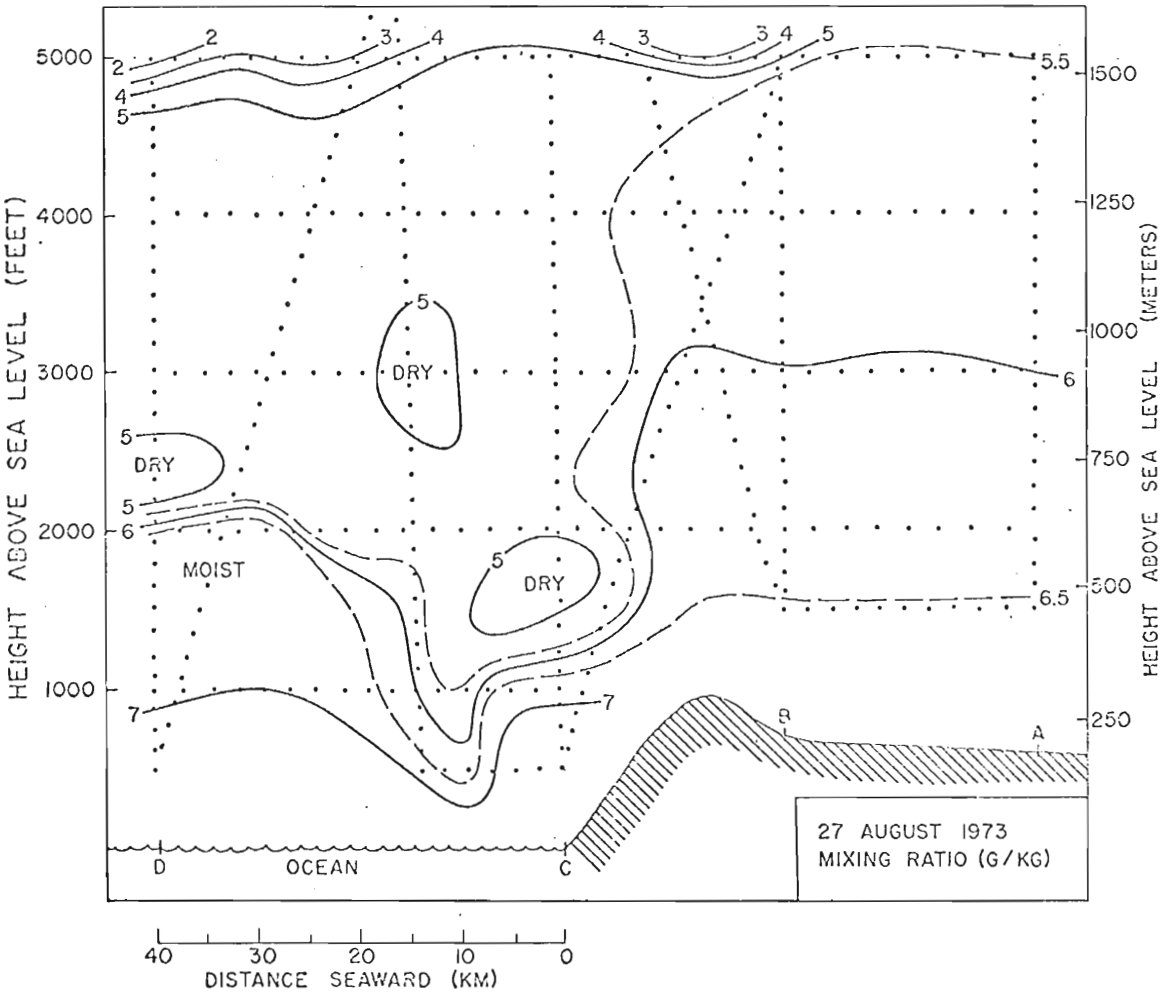

Fig. 21. Cross section of mixing ratio ($g\ kg^{-1}$) for the period 1615-1900 PDT 27 Aug 1973.

The temperature lapse rate was almost dry adiabatic, both inland and seaward, up to an inversion near 1500 m.

With a very smooth ocean surface, aircraft measured winds over the ocean were unreliable, as the Doppler system often went into memory. From the coast inland, pibal and aircraft winds indicate a return flow of the sea breeze circulation between 1000-1500 m. The westerly component of the low level (surface to 750 m) wind increases from the coast inland. Again, as on 26 August, there is some indication that the relatively dry air in the lowest 600 m over the coastal region is associated with the west end of the sea breeze circulation (Fig. 21).

Note the deep protrusion of presumed subsidence from 10-15 km seaward extending almost down to the sea surface. We suggest that similar occurrences produced the offshore subsidence bands, and the corresponding offshore wind speed maximum, observed during the afternoons of 18 August (Fig. 10) and 25 August (Fig. 7). Near the coast, it is speculated that upslope winds counteract the subsidence.

Sea surface temperatures for 27 August are coldest near the coast (11C), increase rapidly to 14C at 8 km seaward, and increase to 16C 30 km seaward. Apparently, the strongest subsidence is not located directly over the coldest water. However, we are <u>not</u> suggesting that there is no relation between the sea surface temperature pattern and the region of subsidence aloft, for the differential heating produced by the cold water and heated interior is an important mechanism in initiating and maintaining the sea breeze circulation. We are only indicating that the region
and heated interior is an important mechanism in initiating and maintaining the sea breeze circulation. We are only indicating that the region
of greatest penetration of presumed subsidence is <u>not directly</u> determined by the sea surface temperature pattern.

c. Case of 1 August

The synoptic scale pattern for 1700 PDT 1 August shows a large anticyclone over the eastern Pacific centered near 140W, 40N and extending northeastward to the Oregon-Washington coast. The sea level coastal pressure pattern is similar to that of 25 August (Fig. 5); but the central Oregon coast pressure is higher (1020 mb), the east-west pressure gradient is stronger, and the thermal gradient is more intense. Consequently, maximum coastal wind speeds at the surface are approximately 12 m sec^{-1} on 1 August, occurring at approximately 1800 PDT, as compared to 8 m sec^{-1} on 25 August.

The vertical cross section for 1 August (Fig. 22) reveals a sharp inversion, which disappears inland. Below the seaward part of the inversion, heavy fog prevented obtaining any flight data.

The top of the marine layer (Fig. 23) coincides approximately with the base of the inversion over the ocean. Sharp drying takes place through the marine inversion. Over land, the combination of convection and orographic effects apparently act to break up the marine inversion.

The winds for 1 August were N-NNW at 12 m sec^{-1} below the inversion. Above the main inversion, the winds decreased to 6-8 m sec^{-1} and were NNE up to 1200 m over the ocean. Inland, it is apparent that the sea breeze circulation has developed, as westerlies extend up to 800 m, switching to easterlies from 800-1100 m. Again, we speculate that the tongue of drier air above the coastal region is associated with the west end of the sea breeze circulation. The sea breeze has not reached Willamette Valley (50 km inland) by this time of day.

end of the sea breeze circulation. The sea breeze has not reached Willamette Valley (50 km inland) by this time of day.

The important feature to note for this case study is that the presumed subsidence does not penetrate the strong marine inversion. The

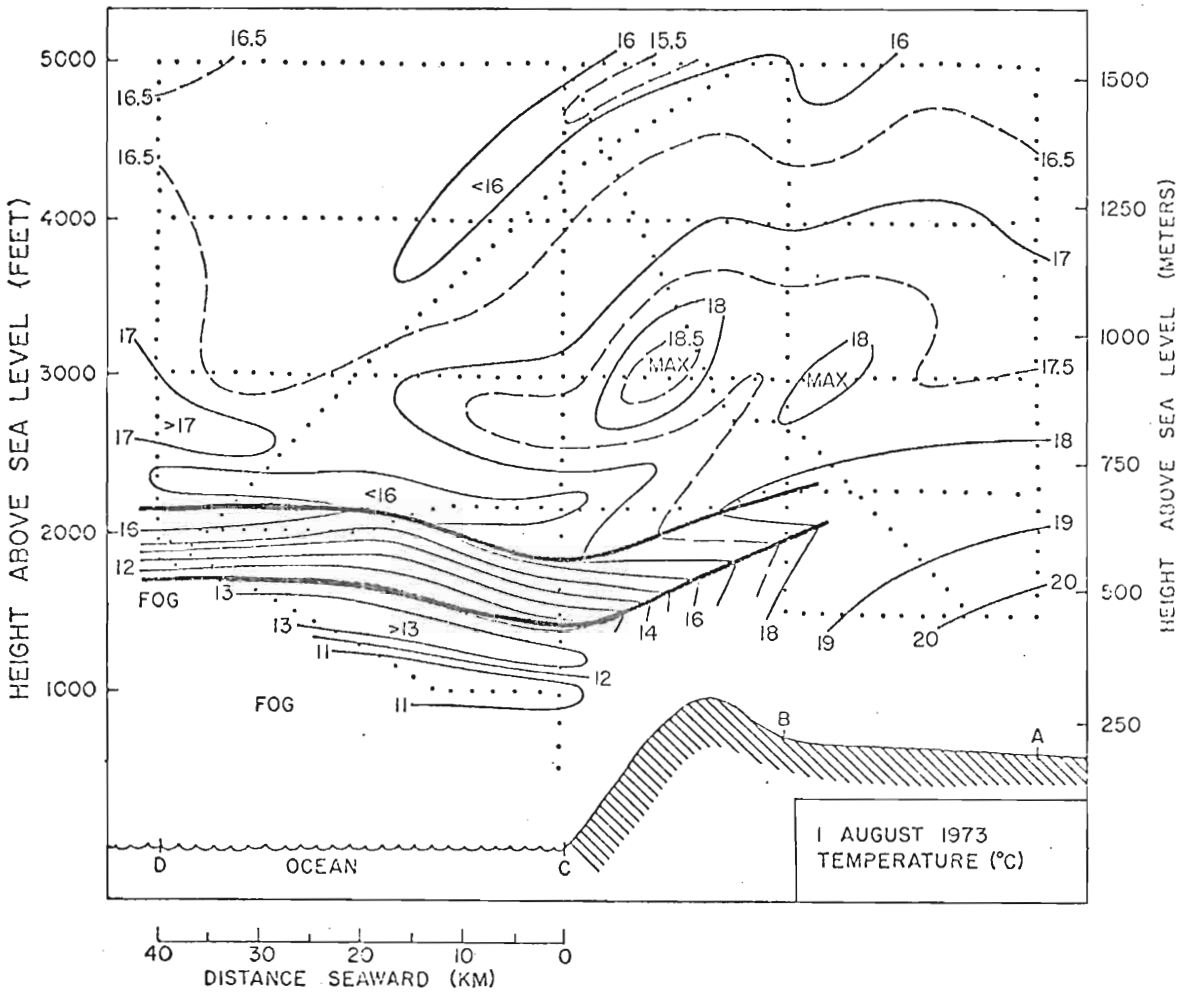

Fig. 22. Temperature cross section for the period 1100-1330 PDT 1 Aug 1973. Dotted lines show the aircraft flight pattern. The heavy solid lines indicate the base and top of the main inversion layer.

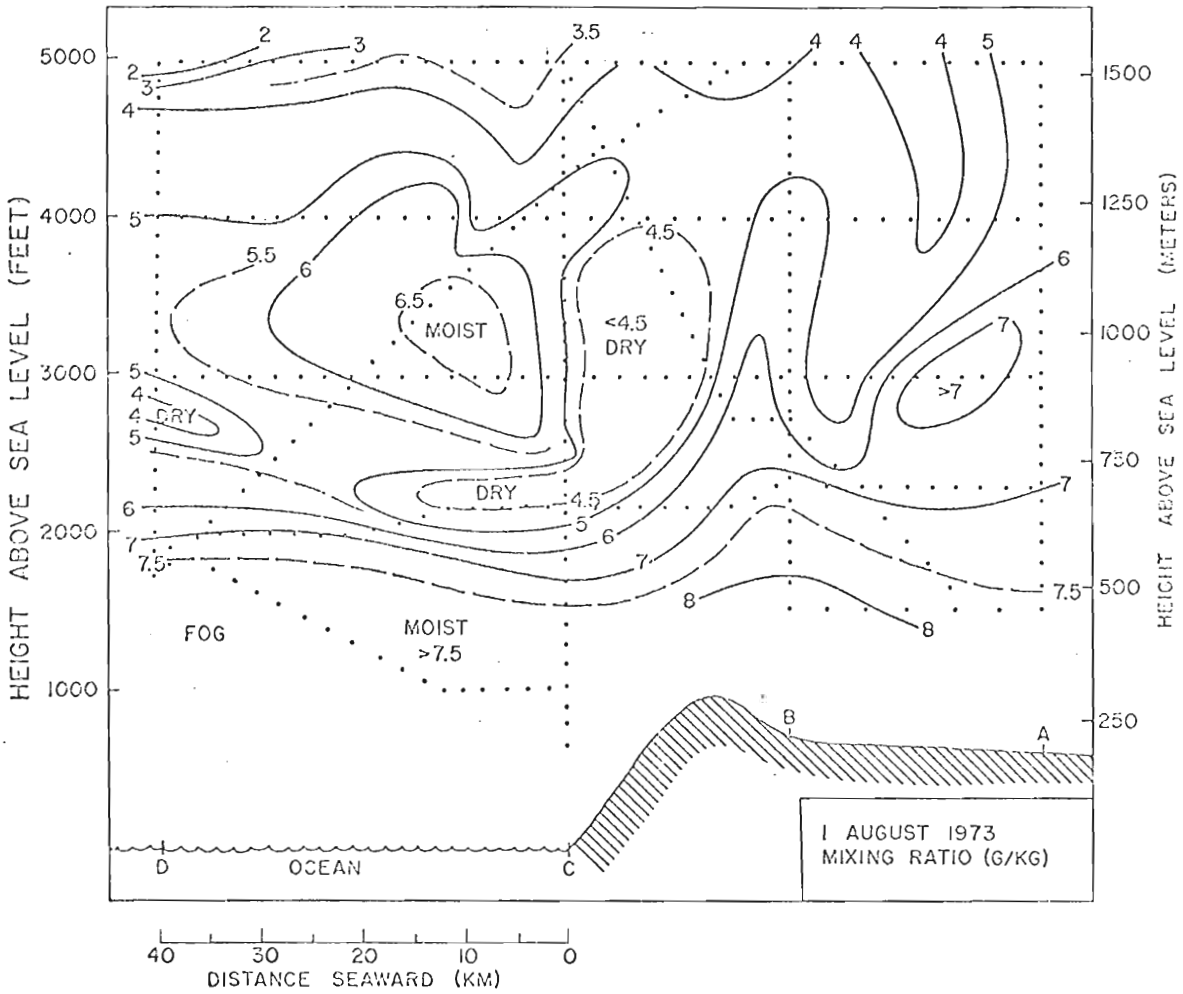

Fig. 23. Cross section of mixing ratio (g kg^{-1}) for the period 1100-1330 PDT 1 Aug 1973.

vertical structure here is very similar to that of 14 August (Fig. 14), which is also characterized by a strong low level marine inversion. The 150 m level winds for 14 August (Figs. 15 and 16) show a decrease of wind speed seaward. Apparently, the subsidence does not penetrate to the extent necessary to provide momentum for an offshore low level wind speed maximum.

The sea surface temperature pattern for 1 August, with coldest water (< 9C) near the coast and increasing to 14C 40 km seaward, is similar to that observed on both 18 August (Fig. 10) and 14 August (Fig. 17).

In summarizing this section, we emphasize the importance of the basic stratification and depth of the marine layer in determining the horizontal and vertical distribution of the low level horizontal wind field over an upwelling region. However, in spite of the basic stratification and depth of the marine layer, a region of coastal subsidence aloft always seems to occur during the afternoon for an upwelling regime and appears to be linked with the west end of the sea breeze circulation.

5. SUMMARY AND CONCLUSIONS

The case studies presented in this paper are believed to exibit the majority of mesoscale features existing in the atmosphere over an upwelling regime for the Oregon coast region. The most outstanding features observed were the offshore low level jet and the tongue of relatively dry air in the vertical which appears to be associated with the west end of the sea breeze circulation. Some important characteristics of the offshore low level jet, with respect to the stratification, depth of the marine layer, sea surface temperature, and sea breeze circulation, are:

1) The low level jet has a structure (or existence) which depends on the basic stratification and the depth of the marine layer.
2) There is no apparent direct relationship between the actual sea surface temperature pattern and the occurrence of the offshore jet observed at the 150 m level.
3) From an investigation of surface buoy and ship winds, there is no evidence of the offshore jet extending down to the sea surface.
4) The offshore jet observed at the 150 m level is strictly a mesoscale phenomenon, with a width scale of 20-30 km, occurring from 10-30 km seaward.
5) A narrow region of subsidence, which appears to be linked to ring from 10-30 km seaward.
5) A narrow region of subsidence, which appears to be linked to the west end of the sea breeze circulation, is suggested to

be a major mechanism in the maintenance of the offshore low level jet.

There is no evidence (from cross sections of mixing ratio) that the sea breeze circulation ever extends further west than 20 km seaward. For the case of a deep marine layer with no low level inversion (Fig. 21), the west end of the sea breeze circulation is apparent over the immediate coast region. Thus we conclude that the sea breeze circulation has only a small seaward extent.

The influence of orographic effects is difficult to infer. Upslope winds along the coast range of mountains would tend to counteract the subsidence from aloft, while downslope winds would tend to increase the strength of the subsidence. It is speculated that upslope winds at the coast may play an important role in preventing offshore low level (150 m) subsidence from occurring any closer to the coast than 10 km seaward.

The uniqueness of this study must not be overlooked, as it is based on the most extensive meteorological investigation ever conducted over a coastal upwelling region. In spite of obvious limitations, the results should give some insight to the understanding of the three dimensional mesoscale structure of the atmosphere during a coastal upwelling regime and, perhaps, stimulate some ideas for future research studies of this nature.

of this nature.

REFERENCES

Bunker, A. F., 1965: A low level jet produced by air, sea, and land interactions. In J. Spar (ed.), Sea-Air Interaction Laboratory Report No. 1. Washington, D. C., p. 225-238.

Burris, R. H., J. C. Covington, and M. N. Zrubek, 1973: Beechcraft Queen Air aircraft. Atmospheric Technology, No. 1, National Center for Atmospheric Research, Boulder, Colo., 25-27.

Burt, W., H. Crew, N. Plutchak, and J. Dumon, 1973: Diurnal variations of winds over an upwelling region off Oregon. (Submitted to Boundary Layer Meteorology.)

_____, D. B. Enfield, R. L. Smith, and H. Crew, 1973: The surface wind over an upwelling region area near Pisco, Peru. Boundary Layer Meteorology, 3, 385-391.

Duchon, C. E., C. J. Biter, C. G. Wade, and P. G. Stickel, 1972: Field calibration and intercomparison of aircraft meteorological systems. Bull. Amer. Meteor. Soc., 53, 1051 (abstract).

Findlater, J., 1972: Aerial explorations of the low-level cross equatorial current over eastern Africa. Quart. J. Roy. Meteor. Soc., 98, 274-289.

Foote, G. B., and J. C. Fankhauser, 1973: Airflow and moisture budget beneath a northeast Colorado hailstorm. J. Appl. Meteor., 12, 1330-1353.

Holladay, C. G., and J. J. O'Brien, 1974: Mesoscale variability of sea surface temperatures. (To be submitted to J. Phys. Oceanogr.)

Johnson, A., and J. J. O'Brien, 1973: A study of an Oregon sea breeze event. J. Appl. Meteor., 12, 1267-1283.

Maeda, S., and R. Kishimoto, 1970: Upwelling off the coast of Peru. J. Oceanogr. Soc. Japan, 26, 300-309.

National Hail Research Experiment, 1972: NHRE Program Plan, 1972-1976. National Center for Atmospheric Research, Boulder, Colo., 132 pp.

National Hail Research Experiment, 1972: NHRE Program Plan, 1972-1976. National Center for Atmospheric Research, Boulder, Colo., 132 pp.

REFERENCES - Continued

O'Brien, J. J., D. L. Elliott, and R. Legeckis, 1974: Sea surface temperature maps from CUE II. CUEA Newsletter, Vol. 3, No. 1, 14-16. Available from Duke University Marine Lab, Beaufort, North Carolina.

Pillsbury, R. D., and J. J. O'Brien, 1973: A summary listing of data collected during Coastal Upwelling Experiment - Phase II (CUE II). Available from School of Oceanography, Oregon State University, Corvallis, Oregon, 120 pp.